Stable and accurate hybrid finite volume methods based on pure convexity arguments for hyperbolic systems of conservation law

Florian De Vuyst *

July 15, 2003

Revised version of the paper proposal JCOMP-D-03-00051 for JCP.

Abstract

This exploratory work tries to present first results of a novel approach for the numerical approximation of solutions of hyperbolic systems of conservation laws. The objective is to define stable and "reasonably" accurate numerical schemes while being free from any upwind process and from any computation of derivatives or mean Jacobian matrices. That means that we only want to perform flux evaluations. This would be useful for "complicated" systems like those of two-phase models where solutions of Riemann problems are hard, see impossible to compute. For Riemann or Roe-like solvers, each fluid model needs the particular computation of the Jacobian matrix of the flux and the hyperbolicity property which can be conditional for some of these models makes the matrices be not $\mathbb{R}$-diagonalizable everywhere in the admissible state space. In this paper, we rather propose some numerical schemes where the stability is obtained using convexity considerations. A certain rate of accuracy is also expected. For that, we propose to build numerical hybrid fluxes that are convex combinations of the second order Lax-wendroff scheme flux and the first order modified Lax-Friedrichs scheme flux with an "optimal" combination rate that ensures both minimal numerical dissipation and good accuracy. The resulting scheme is a central scheme-like method. We will also need and propose a definition of *local dissipation by convexity* for

*Ecole Centrale de Paris, Laboratoire de Mathématiques Appliquées aux Systèmes (MAS), Grande Voie des Vignes, F-92295 Châtenay-Malabry FRANCE, e-mail: devuyst@mas.ecp.fr

hyperbolic or elliptic-hyperbolic systems. This convexity argument allows us to overcome the difficulty of nonexistence of classical entropy-flux pairs for certain systems. We emphasize the systematic feature of the method which can be fastly implemented or adapted to any kind of systems, with general analytical or data-tabulated equations of state.

The numerical results presented in the paper are not superior to many existing state-of-the-art numerical methods for conservation laws such as ENO, MUSCL or central scheme of Tadmor and coworkers. The interest is rather the systematic feature of the method and its very fast implementation for prototypying and fluid model validation. In this context, the Rusanov scheme is often used; the present approach here gives far better results.

Key-Words: Nonlinear hyperbolic systems, conservation laws, finite volume method, hybrid scheme, convexity, entropy, entropy dissipation, upwind-free method, slope-free method, derivative-free method.

AMS Classification: 35L65, 65M06, 65M12, 65Z05, 76M12, 76N15, 76T10.

1 Introduction

We are interested in the approximation of weak solutions of the initial value problem with hyperbolic system of conservation laws

$$\begin{aligned} &\partial_t U + \partial_x F(U) = 0,\ x \in \mathbb{R},\, t \geq 0, \\ &U(x,0) = U^0(x), \end{aligned} \tag{1}$$

where U belongs to an open set of admissible state space $\Omega \subset \mathbb{R}^p$, $p \geq 1$, the flux F has piecewise $\mathcal{C}^1$ regularity on Ω and the initial data $U^0 \in BV(\mathbb{R})$ is given. The hyperbolic assumption means that the Jacobian matrix $A(U) = D_U F(U) \in \mathcal{M}(\mathbb{R}^p)$ is diagonalizable in $\mathbb{R}$ for all $U \in \Omega$ where F is differentiable. Among all the weak solutions, we need to select the physically relevant solution. For that, we suppose that the system of (1) admits some entropy-flux pair (S, Ψ) in the sense given by Lax in [28], that means that, for smooth solutions of (1), the following additional scalar conservation law holds for U:

$$\partial_t S(U) + \partial_x \Psi(U) = 0,\ x \in \mathbb{R},\, t \geq 0. \tag{2}$$

For that, we ask Ψ to satisfy the compatibility relation

$$D_U\Psi(U) \;=\; D_U S(U)\, D_U F(U), \tag{3}$$

where $D_U S(U), D_U\Psi(U) \in \mathcal{L}(\mathbb{R}^p, \mathbb{R})$, $D_U F(U) \in \mathcal{L}(\mathbb{R}^p)$. In what follows, we will use the abuse notation $D_U S(U)$ as either the linear application or its matrix representation, so that, depending on the context, we could also have $D_U S(U), D_U\Psi(U) \in \mathcal{M}_{1,p}(\mathbb{R})$ (row matrix), $D_U F(U) \in \mathcal{M}_p(\mathbb{R})$ (square matrix).
The physically relevant (or entropy) weak solution is expected to satisfy the partial differential inequation

$$\partial_t S(U) + \partial_x \Psi(U) \leq 0,\ x \in \mathbb{R},\, t \geq 0, \tag{4}$$

where this expression is read in the sense of distributions. Notice that, for certain "complicated" hyperbolic systems, we do not known any entropy-flux pair. This is the case for example for the usual six equation two-phase model with one pressure ([16], [22],[10]). Remark that in those cases, the crossing characteristics Lax compatibility conditions [28] allow for selecting the physically relevant solution, that we call again entropy solution. The numerical treament of systems that do not have entropy-flux pairs is also discussed in this paper. We propose an alternative equation to select the physically entropy dissipative solution. It is based on the discretization of the nonconservative equation

$$\partial_t S(U) \;+\; D_U S(U)\, \partial_x F(U) = 0,$$

for a convex function $S(U)$.

Now, we interest us to the numerical approximations of solutions of (1),(4). Let h and τ be respectively two constant space and time steps and $\lambda = \frac{\tau}{h}$ be the ratio of discretisation steps. We are looking for conservative three point difference schemes

$$U_j^{n+1} = U_j^n - \lambda \left(\Phi_{j+\frac{1}{2}}(U_j^n, U_{j+1}^n; \lambda) - \Phi_{j-\frac{1}{2}}(U_{j-1}^n, U_j^n; \lambda) \right) \tag{5}$$

where U_j^n is an approximation of the entropy solution U at position $x_j = jh$ and $t^n = n\tau$ and $\Phi(U, V; \lambda)$ be a numerical flux depending on adjacent states U and V and also on the step ratio λ. The indice $j + \frac{1}{2}$ denotes the interface at position $x_{j+\frac{1}{2}} = (j + \frac{1}{2})h$. In what follows, we will often denote $F_U = F(U)$ or $F_j^n = F(U_j^n)$, $S_j^n = S(U_j^n)$, $\Psi_j^n = \Psi(U_j^n)$ for integer indice j and $\Phi_{j+\frac{1}{2}}^n = \Phi_{j+\frac{1}{2}}^n(U_j^n, U_{j+1}^n; \lambda)$.

The objective of this paper is to decline a class of methods of the form (5) that can fulfil the most of the following requirements:

1. no wave is computed, and thus no upwinding process is applied;

2. no derivative, especially no Jacobian matrix is computed;

3. the method is systematic, that means that its extension from basic modeling to sophisticated modeling (from perfect to real fluid in the Euler context for example) does not require strong analysis and implementation effort;

4. the method is "sufficiently" accurate, with better accuracy in smooth regions of solutions than that of usual first order schemes;

5. the method is stable at the discrete level.

This is motivated by the fact that "complicated" systems lead to either a hard resolution of Riemann problems or a heavy computation of Jacobian matrices, eigenvectors and Riemann invariants. Although alternatives to the treament of strong nonlinearities have been recently proposed by the powerful approach of relaxation schemes ([26], [12]), difficulties of analysis still exist. Relaxation methods require for example a case-by-case heavy study of analysis of sub-characteristic stability performed by entropy compatibility or by Chapman-Enskog-like expansions ([3]). A. In [24] showed that relaxed schemes proposed by Coquel and Perthame [12] are a good way to extend classical schemes of the Euler polytropic gases dynamics in a rather simple, systematic and accurate manner (in the sense that they can finely capture low moving discontinuities). But they are still first order schemes and require additional work (slope reconstruction, etc.) for reaching second order accuracy.

Regarding the strong expectations 1. to 5., the goal *a priori* appears to be hard to reach. Only few known numerical schemes satisfy conditions 1-2-3. For example, the Modified Lax-Friedrichs scheme with numerical flux

$$\Phi^{LF}(U,V;\lambda) = \frac{F_U + F_V}{2} - \frac{1}{4\lambda}(V-U) \tag{6}$$

only needs flux evaluations at cell states. It is proven that this scheme is TVD for scalar conservation laws and it fulfils a discrete entropy inequality for all entropy-flux pairs. But it is well-known that it suffers from an excessive amount rate of numerical dissipation which makes it an irrelevant candidate for reasonably accurate computations.

The two-step Richtmyer Lax-Wendroff scheme [38]

$$\begin{aligned} U_{j+\frac{1}{2}}^{n+\frac{1}{2}} &= \frac{1}{2}\left(U_j^n + U_{j+1}^n\right) - \frac{\lambda}{2}\left(F_{j+1}^n - F_j^n\right), \\ U_j^{n+1} &= U_j^n - \lambda\left(F(U_{j+\frac{1}{2}}^{n+\frac{1}{2}}) - F(U_{j-\frac{1}{2}}^{n+\frac{1}{2}})\right), \end{aligned}$$

as well as the MacCormack scheme [32] also only require flux evaluations. Notice that Benkhaldoun [1] recently proposed a variant of the Richtmyer Lax-Wendroff scheme adapted to nonhomogeneous systems of conservation laws that ensures TVB stability. He tested his scheme on the Ransom's faucet problem and obtained very promising results. Finally, the Lax-Wendroff scheme [29] with numerical flux

$$\Phi^{LW}(U,V;\lambda) = \frac{F_U + F_V}{2} - \frac{\lambda}{2}\bar{A}(U,V)(F_V - F_U), \tag{7}$$

where matrix $\bar{A}(.,.)$ is such that $\bar{A}(U,U) = A(U)$, is the unique three point scheme which is second order accurate in both space and time. It is linearly L^2-stable, but suffers from a lack of numerical dissipation especially at sonic points, that makes it an strongly oscillatory scheme that generally violates the entropy property. It has even been proved to be nonlinearly unstable near stagnation points (see Majda-Osher [33]). Although the Lax-Wendroff scheme does not need to select upwind and downwind information, it nevertheless requires the computation of a mean "Jacobian" matrix. But, because $\bar{A}$ is applied to the direction $(F_V - F_U)$, it only requires a directional derivative if $\bar{A}(U,V)$ is chosen as $\bar{A}(U,V) = A(\bar{\varphi}(U,V))$ where the mean state function $\varphi(U,V)$ satisfies the consistency relation $\varphi(U,U) = U$. More, Lax-Wendroff flux can be approximated as close as wanted by the class of one-parameter fluxes of parameter $\epsilon \in \mathbb{R}$ that we denote $\Phi^{LW,\epsilon}$ and define as

$$\Phi^{LW,\epsilon}(U,V;\lambda) = \frac{F_U + F_V}{2} - \frac{\lambda}{2}\,\frac{F\left[\bar{\varphi}(U,V) + \epsilon(F_V - F_U)\right] - F(\bar{\varphi}(U,V))}{\epsilon}, \tag{8}$$

where ϵ is intented to be a "small" parameter. Thus, we do not need to compute any derivative. At our knowledge, this has not never been remarked. This numerical flux is bounded if the physical flux F is only locally Lipschitz continuous.

We could also mention the numerical flux of the Rusanov scheme [40]

$$\Phi^{R}(U,V) = \frac{F_U + F_V}{2} - \frac{1}{2}\,\sigma_{max}(U,V)(V - U),$$

where the scalar $\sigma_{max}(U,V) \geq 0$ is an estimate of local largest velocity of propagation of waves that are generated by some Riemann problems of initial data (U,V). In its original form, Rusanov proposed for

estimating σ_{max}

$$\sigma_{max}(U,V) \;=\; \frac{1}{2}\{|\lambda|_{max}(U)+|\lambda|_{max}(V)\},$$

where $|\lambda|_{max}(U)$ is the largest propagation velocity of state U. Notice that, in general, physical considerations are sufficient to find the largest velocity so it is not necessary to compute the eigenvalues of the Jacobian matrix of the flux. Indeed, with physical systems, it is quite usual to deal with maximum propagation velocities of the form $|u|+c$, where u is the fluid velocity and c is some "speed of sound". As a consequence, the Rusanov scheme is often used in applications but still suffers from an excessive amount of numerical dissipation. Notice that the need to know the largest propagation velocity is also necessary for any numerical explicit scheme because of the Courant-Friedrich-Lewy (CFL) stability condition of the form

$$\lambda \sup_{j\in\mathbb{Z}}(\sigma_{max}(U_j^n,U_{j+1}^n)) \;\leq\; \beta, \tag{9}$$

for some β, $0<\beta\leq 1$ at each time step $t^n=n\tau$.

The complementary advantages of both Modified Lax-Wendroff and Lax-Friedrichs schemes invite us to explore an hybrid numerical flux of the form

$$\phi^{\epsilon}_{j+\frac{1}{2}} \;=\; \theta_{j+\frac{1}{2}}\Phi^{LF}_{j+\frac{1}{2}} \;+\; (1-\theta_{j+\frac{1}{2}})\Phi^{LW,\epsilon}_{j+\frac{1}{2}}, \tag{10}$$

for a local scalar real $\theta_{j+\frac{1}{2}}$, $0\leq\theta_{j+\frac{1}{2}}\leq 1$. The question is to find the "optimal" value for $\theta_{j+\frac{1}{2}}$. In classical hybridation, second-order flux limitations are considered using *minmod*-like limiters (see Halaoua [16] for hybridation in the two-phase flow context). For a recent construction of an accurate entropy-satisfying hybrid scheme, the reader can refer to Bouchut [6].

In what follows, we will consider quantities $\theta^n_{j+\frac{1}{2}}$ as functions of states U^n_{j-1}, U^n_j, U^n_{j+1} and U^n_{j+2} with possible dependency on parameter λ (the dependency to the fixed parameter ϵ will not be mentioned for the sake of simplicity of script):

$$\theta^n_{j+\frac{1}{2}}=\theta^n_{j+\frac{1}{2}}(U^n_{j-1},U^n_j,U^n_{j+1},U^n_{j+2};\lambda). \tag{11}$$

The strategy proposed in this paper is to estimate what we call local numerical dissipation by convexity and calibrate the sequences $(\theta^n_{j+\frac{1}{2}})_{j\in\mathbb{Z}}$ in such a way that the two following constraints are respected:

1. each local discrete dissipation by convexity is negative;

2. coefficient $\theta^n_{j+\frac{1}{2}}$ is as close to zero as possible (the numerical flux is as close to the second order Lax-Wendroff flux as possible).

The paper is structured as follows : in section 2, we propose a numerical tool to estimate the local numerical dissipation associated to a given numerical scheme within a cell. This will be useful in section 3 to propose a conservative hybrid scheme that "optimizes" the rate of numerical dissipation. In section 4, it is discussed natural extensions of the scheme to the case of systems with nonconservative products and source terms. Finally in section 5, we will perform several numerical tests on both one space and two space dimensions and also for nonhomogeneous and non conservative systems (two-phase flows).

2 The approximate Lax-Wendroff flux

In the introduction, we have discussed about an approximation of the Lax-Wendroff flux that avoids the computation of a mean Jacobian matrix and only performs flux evaluations; this is interesting for the point of view of the computational effort and for the systematic feature of the method. For that, we use a numerical approximation of a directional derivative and a parameter ϵ. Recall that the approximate flux has the form

$$\Phi^{LW,\epsilon}(U,V;\lambda) = \frac{F_U + F_V}{2} - \frac{\lambda}{2}\frac{F\left[\bar{\varphi}(U,V) + \epsilon(F_V - F_U)\right] - F(\bar{\varphi}(U,V))}{\epsilon}, \tag{12}$$

In this section, we give indications concerning the choice of parameter ϵ in practice and the possible loss of accuracy generated by the relaxation parameter. The first remark is that, by chosing $\epsilon = -\frac{\lambda}{2}$ and $\bar{\varphi}(U,V) = \frac{U+V}{2}$, we find out a variant of the Richtmyer Lax-Wendroff flux:

$$\Phi^{LW,-\frac{\lambda}{2}}(U,V) \;=\; F\left(\frac{U+V}{2} - \frac{\lambda}{2}\left(F_V - F_U\right)\right) + \frac{F_U + F_V}{2} - F\left(\frac{U+V}{2}\right). \tag{13}$$

Let us make some short comments about this script. We retrieve the original term of the original Lax-Wendroff Richtmyer original flux and an additional difference term

$$\frac{F_U + F_V}{2} - F\left(\frac{U+V}{2}\right).$$

This term somewhat changes the behaviour of the original scheme. In particular, stationary contact discontinuities are preserved. However, the added difference term is of second order.

For a (small) arbitrary value of ϵ, denoting by $\bar{U} = \frac{U+V}{2}$ and $\Delta F = F_V - F_U$, an exact Taylor expansion under integral form shows that

$$\begin{aligned}\Phi^{LW,\epsilon}(U,V) &= F(\bar{U}) - \frac{\lambda}{2}A(\bar{U})\Delta F - \frac{\lambda\epsilon}{2}\int_0^1 (1-s)D^2F(\bar{U}+\epsilon s\Delta F)\,ds\ (\Delta F,\Delta F).\\ &= \Phi^{LW}(U,V) - \frac{\lambda\epsilon}{2}\int_0^1 (1-s)D^2F(\bar{U}+\epsilon s\Delta F)\,ds\ (\Delta F,\Delta F).\end{aligned}$$

Denoting by $\mathcal{T}$ the tensor

$$\mathcal{T} = \int_0^1 (1-s)D^2F(\bar{U}+\epsilon s\Delta F)\,ds,$$

we have the estimate

$$||\Phi^{LW,\epsilon}(U,V) - \Phi^{LW}(U,V)|| \leq \frac{1}{2}\lambda\,|\epsilon|\,|||\mathcal{T}|||_{\mathcal{L}(\mathcal{L}(\mathbb{R}^p);\mathcal{L}(\mathbb{R}^p))}\,||\Delta F||^2.$$

Consequently, while $|\epsilon|$ is bounded by a constant $\epsilon^\star$, the right hand side is $O(||\Delta U||^2)$ and then of second order, so that the relaxation process does not make the scheme more diffusive. This estimate also shows that, if F is linear, there is no difference between Φ^{LW} and $\Phi^{LW,\epsilon}$. About the behaviour of the approximate Lax-Wendroff scheme through discontinuities, we have tested numerical experiments on the scalar inviscid Burgers equation

$$\partial_t u + \partial_x(u^2/2) = 0.$$

Let us consider a shock tube problem on the interval $]0,1[$ with initial discontinuity at 0.5, left state $u_l = 1$ and right state $u_r = 0$. We did computations with the respective constant values of ϵ: $\epsilon = 10^{-6}$, -10^{-6} and variable values $\epsilon = -\frac{\lambda^n}{4}$ and $-\frac{\lambda^n}{2}$ at each time t^n. We also compare results with the original Lax-Wendroff scheme. Figure 1 shows the results using a CFL number equal to 0.5 and a uniform mesh using 100 mesh points. We can conclude that the numerical solution is not sensible to the choice of ϵ and the results are very close to those obtained by the original Lax-Wendroff scheme. Of course, the numerical solution is oscillatory: it is well-known that the Lax-Wendroff scheme is not TVD and produces oscillations through discontinuities. As an independent remark, we have performed a computation using the big value $\epsilon = -10$ and surprisingly remarked that the oscillations at the head of the shock are smaller (see the figure). A computation with $\epsilon = +10$ breaks down. A choice of negative value for ϵ is thus recommended.

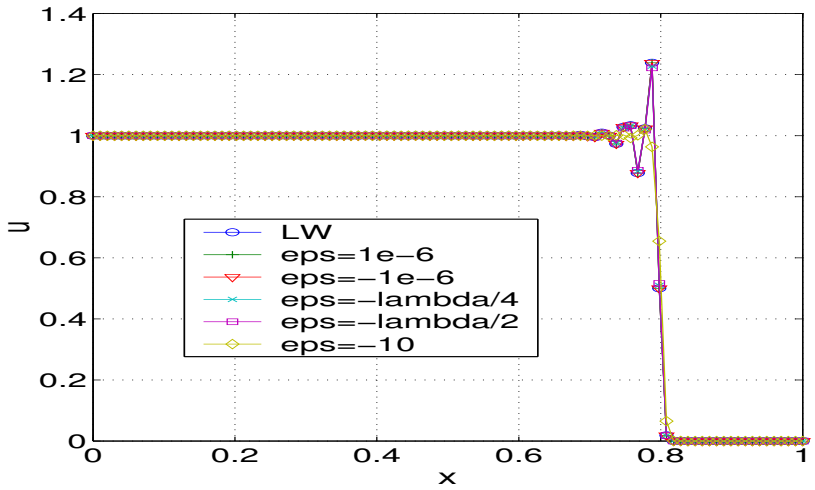

Figure 1: Comparison between Lax-Wendroff and approximate Lax-Wendroff for different values of ϵ: 10^{-6}, -10^{-6}, $-\frac{1}{4}\lambda^n$, $-\frac{1}{2}\lambda^n$ and -10 (the scheme breaks down for $\epsilon = 10$).

3 Investigating expressions of local discrete entropy dissipation

An interesting way to calibrate the combination coefficients $\theta^n_{j+\frac{1}{2}}$ is to locally control the amount of numerical entropy dissipation. So we do a brief introduction on local discrete entropy inequalities.

Discrete versions of the partial differential inequality (4) are of the form

$$\eta_j^{n+1} = S_j^{n+1} - S_j^n + \lambda \left(\Psi^n_{j+\frac{1}{2}} - \Psi^n_{j-\frac{1}{2}} \right), \tag{14}$$

where $\Psi^n_{j+\frac{1}{2}} = \Psi(U_j^n, U_{j+1}^n)$ is a Lipschitz continuous numerical entropy flux that respects the consistency property $\Psi(U,U) = \Psi(U)$. The quantity η_j^{n+1} gives an estimate of the amount of numerical dissipation per cell j between times t^n and t^{n+1} and is expected to be less or equal to zero. In the case of the Godunov scheme ([14]), it is easy to find the numerical entropy flux. Let us recall that the Godunov flux $\Phi_{j+\frac{1}{2}}$ is sought as the physical flux of the solution $U_{Riem}(x_{j+\frac{1}{2}}; U_j^n, U_{j+1}^n)$ of the local Riemann problem of initial states (U_j^n, U_{j+1}^n) at interface $x_{j+\frac{1}{2}} = (j+\frac{1}{2})h$. Under convenient CFL condition that forbids the interaction of neighbouring waves, let us integrate (4) on the cell $]x_{j-\frac{1}{2}}, x_{j+\frac{1}{2}}[\times]t^n, t^{n+1}[$. Then it is easy to show that one obtains (14) with the following numerical entropy flux:

$$\Psi^n_{j+\frac{1}{2}} = \Psi(U_{Riem}(x_{j+\frac{1}{2}}; U_j^n, U_{j+1}^n)).$$

Unfortunately, for other numerical fluxes, we do not generally know the numerical entropy flux associated to the numerical flux. Approximate Riemann solvers and kinetic schemes are particular families of schemes where the numerical entropy flux can be exhibited.

In the general case, some authors have proposed alternative computational formulae to estimate entropy dissipation without the knowledge of the numerical entropy flux. For example, Coquel and Liou [9] have suggested to perform a balance of entropy dissipation not inside a cell as usual, but at a cell interface $x_{j+\frac{1}{2}}$. Let us rapidly recall the construction. We define two adjacent new states $U^{n+1}_{j+\frac{1}{2},-}$ and $U^{n+1}_{j+\frac{1}{2},+}$ on respective intervals $]x_j, x_{j+\frac{1}{2}}[$ and $]x_{j+\frac{1}{2}}, x_{j+1}[$ by

$$U^{n+1}_{j+\frac{1}{2},-} = U^n_j - 2\lambda\left(\Phi^n_{j+\frac{1}{2}} - F^n_j\right), \tag{15}$$

$$U^{n+1}_{j+\frac{1}{2},+} = U^n_j - 2\lambda\left(F^n_{j+1} - \Phi^n_{j+\frac{1}{2}}\right). \tag{16}$$

Then we can show expressions of numerical entropy dissipation on each half cell $]x_j, x_{j+\frac{1}{2}}[\times]t^n, t^{n+1}[$ and $]x_{j+\frac{1}{2}}, x_{j+1}[\times]t^n, t^{n+1}[$ ($\Psi^n_{j+\frac{1}{2}}$ is still supposed to be unknown):

$$\eta^{n+1}_{j+\frac{1}{2},-} = S(U^{n+1}_{j+\frac{1}{2},-}) - S^n_j + 2\lambda\left(\Psi^n_{j+\frac{1}{2}} - \Psi^n_j\right), \tag{17}$$

$$\eta^{n+1}_{j+\frac{1}{2},+} = S(U^{n+1}_{j+\frac{1}{2},+}) - S^n_{j+1} + 2\lambda\left(\Psi^n_{j+1} - \Psi^n_{j+\frac{1}{2}}\right). \tag{18}$$

Summing up the two last expressions and dividing by 2 gives the local entropy dissipation per interface

$$\eta^{n+1}_{j+\frac{1}{2}} = \frac{1}{2}\left\{S(U^{n+1}_{j+\frac{1}{2},-}) + S(U^{n+1}_{j+\frac{1}{2},+})\right\} - \frac{1}{2}\left\{S^n_j + S^n_{j+1}\right\} + \lambda\left(\Psi^n_{j+1} - \Psi^n_j\right), \tag{19}$$

where the unknown flux $\Psi^n_{j+\frac{1}{2}}$ disappears. Although this tool is powerful for analyzing numerical dissipation, this still does not give a balance inside a whole cell.

In this paper, we propose an alternative for the computation of what we call *numerical dissipation by convexity*. This terminology is justified below.

This estimate is performed inside a whole cell and not through an interface. As first step, suppose that we deal with a smooth solution. We can rewrite the entropy conservation law (2) under a nonconservative form:

$$\partial_t S(U) + D_U S(U)\,\partial_x F(U) = 0. \tag{20}$$

We then denote the row vector $G(U) = D_U S(U)$. Integrating equation (20) on the cell $]x_{j-\frac{1}{2}}, x_{j+\frac{1}{2}}[\times]t^n, t^{n+1}[$ leads to the following expression of numerical entropy dissipation (see figure 2):

$$\eta_j^{n+1} = S(U_j^{n+1}) - S(U_j^n) + \lambda \left\{ G^n_{j-\frac{1}{2}} \left(F_j^n - \Phi^n_{j-\frac{1}{2}} \right) + G^n_{j+\frac{1}{2}} \left(\Phi^n_{j+\frac{1}{2}} - F_j^n \right) \right\}, \tag{21}$$

where $G^n_{j+\frac{1}{2}} = G(U_j^n, U_{j+1}^n)$ and function $G(.,.)$ is consistent with $G(.)$, that means $G(U,U) = G(U)$ for all U in Ω. We decide to use this terminology rather than numerical entropy dissipation for two reasons :

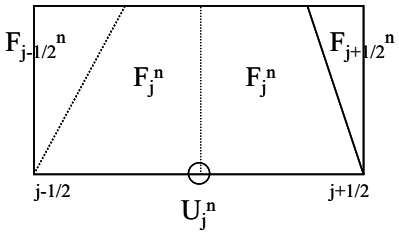

Figure 2: Construction of expression (21) from the sum of nonconservative terms inside cell j.

1. As we will see, although the proposed estimate is expected to be negative, the constraint will be shown to be relaxed compared to the true local entropy dissipation estimate (with possible entropy violation).

2. Because there is no entropy flux in this expression, we do not need the compatibility relation (3), this can be simply applied to any convex function $S(U)$ without the existence of an associated entropy flux.

In what directly follows, we are going to prove that, at least for the Modified Lax-Wendroff scheme, the local discrete convexity dissipation term is negative under appropriate Courant-Friedrichs-Lewy conditions. We begin to investigate it using the simple energy norm $S(U) = \frac{1}{2}||U||^2$, and then discuss further for any convex function $S(U)$.

Proposition 1 *Let us define $S(U) = \frac{1}{2}||U||^2$ and the energy-norm local dissipation term associated to the numerical scheme (5):*

$$\eta_j^{n+1} \;=\; S(U_j^{n+1}) - S(U_j^n) + \lambda \left\{ D_U S^n_{j-\frac{1}{2}} \left(F_j^n - \Phi^n_{j-\frac{1}{2}} \right) + D_U S^n_{j+\frac{1}{2}} \left(\Phi^n_{j+\frac{1}{2}} - F_j^n \right) \right\} \tag{22}$$

with the notation $D_U S^n_{j+\frac{1}{2}} = D_U S \left(\frac{U_j^n + U_{j+1}^n}{2} \right) \in \mathcal{M}_{1,p}(\mathbb{R})$. Suppose that the hyperbolic system of (1) has an entropy-flux pair. We denote by $\bar{A}(U,V)$ a Roe matrix linearization associated to the Jacobian matrix

$D_U F(U)$ for any $U, V \in \Omega^2$. Then, for the numerical flux of the modified Lax-Friedrichs scheme, and under the Courant-Friedrichs-Lewy (CFL) condition

$$\lambda \sup_{j\in\mathbb{Z}} \max_{k\in\{1,\dots p\}} |\lambda_k(\bar{A}(U_j^n, U_{j+1}^n))| \ \leq \ \frac{1}{2}, \tag{23}$$

the following inequality holds:

$$\eta_j^{n+1} \ \leq \ 0 \quad \forall j \in \mathbb{Z}. \tag{24}$$

Proof. As in [9], we introduce two states related to the cell j:

$$U_{j+\frac{1}{2},-}^{n+1} \ = \ U_j^n - 2\lambda \left(\Phi_{j+\frac{1}{2}}^n - F_j^n\right), \tag{25}$$

$$U_{j-\frac{1}{2},+}^{n+1} \ = \ U_j^n - 2\lambda \left(F_j^n - \Phi_{j-\frac{1}{2}}^n\right). \tag{26}$$

Notice that from (5), we have

$$U_j^{n+1} \ = \ \frac{1}{2}\left\{U_{j-\frac{1}{2},+}^{n+1} + U_{j+\frac{1}{2},-}^{n+1}\right\}. \tag{27}$$

We now interest us to have an estimate of the term $D_U S_{j+\frac{1}{2}}^n \left(\Phi_{j+\frac{1}{2}}^n - F_j^n\right)$. By multiplying (25) by $D_U S_{j+\frac{1}{2}}^n$, we get,

$$D_U S_{j+\frac{1}{2}}^n \left(U_{j+\frac{1}{2},-}^{n+1} - U_j^n\right) \ = \ -2\lambda\, D_U S_{j+\frac{1}{2}}^n \left(\Phi_{j+\frac{1}{2}}^n - F_j^n\right).$$

In what follows, we denote $U_{j+\frac{1}{2}}$ the mean value $\frac{1}{2}(U_j^n + U_{j+1}^n)$, $S_{j+\frac{1}{2}} = S(U_{j+\frac{1}{2}})$ and we use the fact that S is quadratic, in particular $D_U S(U) = U^T$, $D_{UU}^2 S(U) = I_p$ and

$$\begin{aligned} S(U_{j+\frac{1}{2},-}^{n+1}) \ &= \ S_{j+\frac{1}{2}} + D_U S_{j+\frac{1}{2}}^n \left(U_{j+\frac{1}{2},-}^{n+1} - U_{j+\frac{1}{2}}\right) + \frac{1}{2}||U_{j+\frac{1}{2},-}^{n+1} - U_{j+\frac{1}{2}}||^2, \\ S_j^n \ &= \ S_{j+\frac{1}{2}} + D_U S_{j+\frac{1}{2}}^n \left(U_j^n - U_{j+\frac{1}{2}}\right) + \frac{1}{2}||U_j^n - U_{j+\frac{1}{2}}||^2. \end{aligned}$$

Then we have

$$S(U_{j+\frac{1}{2},-}^{n+1}) - S_j^n + 2\lambda\, D_U S_{j+\frac{1}{2}}(\Phi_{j+\frac{1}{2}}^n - F_j^n) \ = \ \frac{1}{2}\,||\frac{U_{j+1}^n - U_j^n}{2} + 2\lambda\,(\Phi_{j+\frac{1}{2}}^n - F_j^n)||^2 - \frac{1}{2}\,||\frac{U_{j+1}^n - U_j^n}{2}||^2.$$

The RHS is of the form $\frac{1}{2}(x+h, x+h) - \frac{1}{2}(x,x) = (x + \frac{1}{2}h, h)$, or again

$$\text{RHS} = \left(\frac{U_{j+1}^n - U_j^n}{2} + \lambda(\Phi_{j+\frac{1}{2}}^n - F_j^n),\, 2\lambda\,(\Phi_{j+\frac{1}{2}}^n - F_j^n)\right).$$

Recall that the Modified Lax-Friedrichs numerical flux is

$$\Phi_{j+\frac{1}{2}}^{MLF,n} \ = \ \frac{F_j^n + F_{j+1}^n}{2} \ - \ \frac{1}{4\lambda}\left(U_{j+1}^n - U_j^n\right),$$

so that the RHS becomes in this case

$$\begin{aligned} 2\,\mathrm{RHS} &= 4\,\left(\lambda\frac{F^n_{j+1}-F^n_j}{2}+\frac{1}{4}(U^n_{j+1}-U^n_j),\,\lambda\frac{F^n_{j+1}-F^n_j}{2}-\frac{1}{4}(U^n_{j+1}-U^n_j)\right), \\ &= \lambda^2||F^n_{j+1}-F^n_j||^2-\frac{1}{4}||U^n_{j+1}-U^n_j||^2. \end{aligned}$$

Because the system has an entropy-flux pair, it admits a Roe matrix linearization (Harten and Lax [17]), so that we express again the RHS as

$$\begin{aligned} 2\,\mathrm{RHS} &= \lambda^2||\bar{A}(U^n_j,U^n_{j+1})\left(U^n_{j+1}-U^n_j\right)||^2-\frac{1}{4}||U^n_{j+1}-U^n_j||^2 \qquad (28) \\ &\leq \left(\lambda^2\,||\bar{A}(U^n_j,U^n_{j+1})||^2-\frac{1}{4}\right)\,||U^n_{j+1}-U^n_j||^2. \qquad (29) \end{aligned}$$

Harten and Lax [17] build the Roe matrix linearization as the product of two symmetric matrices, so that it is itself symmetric for a certain choice of variable representation. Consequently,

$$||\bar{A}||_2 \;=\; \rho(\bar{A})$$

where $\rho(\bar{A})$ is the spectral radius of $\bar{A}$. Then from (29) it is clear that if $\rho(\bar{A})\leq\frac{1}{2}$, the right hand side is negative and we get

$$S(U^{n+1}_{j+\frac{1}{2},-})-S^n_j+2\lambda\,D_U S_{j+\frac{1}{2}}(\Phi^n_{j+\frac{1}{2}}-F^n_j)\;\leq\;0. \qquad (30)$$

Under similar CFL condition, we could also prove that

$$S(U^{n+1}_{j-\frac{1}{2},+})-S^n_j+2\lambda\,D_U S_{j-\frac{1}{2}}(F^n_j-\Phi^n_{j-\frac{1}{2}})\;\leq\;0. \qquad (31)$$

Summing up inequalities (30) and (31) gives under $CFL\leq\frac{1}{2}$,

$$\frac{1}{2}\left\{S(U^{n+1}_{j+\frac{1}{2},-})+S(U^{n+1}_{j-\frac{1}{2},+})\right\}-S^n_j+\lambda\,\left\{D_U S^n_{j-\frac{1}{2}}\left(F^n_j-\Phi^n_{j-\frac{1}{2}}\right)+D_U S^n_{j+\frac{1}{2}}\left(\Phi^n_{j+\frac{1}{2}}-F^n_j\right)\right\}\;\leq\;0.$$

Finally because function S is convex and from (27) we have

$$S^{n+1}_j\;\leq\;\frac{1}{2}\left\{S(U^{n+1}_{j+\frac{1}{2},-})+S(U^{n+1}_{j-\frac{1}{2},+})\right\},$$

that gives the expected result.

Remark 1 *1. The proposition introduces Roe matrix linearizations for rigorous script of the CFL condition. But for numerical implementation purposes, this is not necessary. We claim that the knowledge of the largest propagation velocity of each state U^n_j is sufficient to respect a $CFL\leq\frac{1}{2}$-like condition.*

Below, we show that similar results holds for general convex functions $S(U)$, but we cannot write explicitly the CFL criterion for which the local discrete convexity dissipation term is always negative.

Proposition 2 *For any convex function $S(U)$, let us again consider the local dissipation term (22) associated to the modified Lax-Friedrichs scheme. Then the following inequality*

$$\eta_j^{n+1} \ \leq \ 0 \quad \forall j \in \mathbb{Z}. \tag{32}$$

holds for a certain (not in closed form) CFL condition, more restrictive than (23).

Proof. We follow the same ideas of the previous proof, so that we skip some details. Keeping the same notations, we here use exact Taylor expansion under integral form:

$$\begin{aligned} & S(U_{j+\frac{1}{2},-}^{n+1}) \ - \ S_{j+\frac{1}{2}} - D_U S_{j+\frac{1}{2}}(U_{j+\frac{1}{2},-}^{n+1} - U_{j+\frac{1}{2}}) \\ & \stackrel{\text{def}}{=} (R1) \ = \ \int_0^1 (1-t) D_{UU}^2 (U_{j+\frac{1}{2}} + t(U_{j+\frac{1}{2},-}^{n+1} - U_{j+\frac{1}{2}}))\, dt < U_{j+\frac{1}{2},-}^{n+1} - U_{j+\frac{1}{2}}, U_{j+\frac{1}{2},-}^{n+1} - U_{j+\frac{1}{2}} >, \end{aligned}$$

and also

$$\begin{aligned} & S_j^n \ - \ S_{j+\frac{1}{2}} - D_U S_{j+\frac{1}{2}}(U_j^n - U_{j+\frac{1}{2}}) \\ & \stackrel{\text{def}}{=} (R2) \ = \ \int_0^1 (1-t) D_{UU}^2 (U_{j+\frac{1}{2}} + t(U_j^n - U_{j+\frac{1}{2}}))\, dt < U_j^n - U_{j+\frac{1}{2}}, U_j^n - U_{j+\frac{1}{2}} > . \end{aligned}$$

By substraction, and following the previous proof, we get

$$S(U_{j+\frac{1}{2},-}^{n+1}) - S_j^n + 2\lambda D_U S_{j+\frac{1}{2}}(\Phi_{j+\frac{1}{2}}^n - F_j^n) \ = \ (R1) \ - \ (R2).$$

We want the RHS to be negative. For the Modified Lax-Friedrichs scheme, we have

$$\begin{aligned} U_{j+\frac{1}{2},-}^{n+1} - U_{j+\frac{1}{2}} \ &= \ U_j^n - 2\lambda \left[\frac{F_{j+1}^n - F_j^n}{2} - \frac{1}{4\lambda}(U_{j+1}^n - U_j^n) \right] - \frac{1}{2}\left(U_j^n + U_{j+1}^n\right) \\ &= \ -\lambda \left(F_{j+1}^n - F_j^n\right) \end{aligned}$$

and allows us to conclude. Indeed, remark first that if the symmetric matrix $D_{UU}^2 S(U)$ is positive definite for all U, then $(R1)$ and $(R2)$ are positive terms. Secondly, as functions of the variable λ, we remark that $(R1) = O(\lambda^2)$ and $(R2) = O(1)$. Thus, we can choose λ small enough such that the Right Hand Side becomes negative. Notice that we cannot explicitely write the CFL condition, what can be a limitation for practical utilization. The CFL condition is at least required because we expect waves from neighbouring interfaces not to interact. That ends the proof of the proposition.

3.1 Trying to reach conservative forms

As already remarked, expression (21) is written under a nonconservative form. For theoretical purposes, it could be interesting to try to find criteria that can make the convexity dissipation term have a conservative form. If it were possible, this could lead to a true entropy dissipation term.

The first natural idea is to extend Roe linearization ideas not between state and flux jumps but between flux jumps and entropy flux jumps. Suppose that there exists a continuous mean row vector-valued function $G(.,.)$ that satisfies both following consistency and compatibility formulae:

$$G(U,U) \;=\; D_U S(U) \;\; \forall U \in \Omega, \tag{33}$$

$$\Psi(V) - \Psi(U) \;\leq\; G(U,V)\,(F(V) - F(U)) \;\; \forall U, V \in \Omega. \tag{34}$$

Of course, previous expression (34) is consistent with the entropy flux compatibility formula (3). Expression (34) can indeed be in mirror with the well-known Roe compatibility condition for mean Roe matrices $A(U,V)$:

$$F(V) - F(U) \;=\; A(U,V)\,(V-U)\,.$$

This allows us to replaces the nonlinear waves of the original system by waves of a locally linearized one while keeping the interpretation of the Roe scheme as a conservative Godunov-type one (with exact solutions projected on the constants at each time steps t^{n+1}, see [39]). Then we have the following result:

Proposition 3 *Let us consider a Lax entropy pair (S,Ψ). Suppose that there exists a continuous row vector-valued function $G(.,.)$ such that inequality (34) holds. Let $\Psi^n_{j+\frac{1}{2}} = \Psi(U^n_j, U^n_{j+1})$ be a quantity such that*

$$\Psi^n_{j+1} - G(U^n_j, U^n_{j+1})\left(F^n_{j+1} - \Phi^n_{j+\frac{1}{2}}\right) \;\leq\; \Psi^n_{j+\frac{1}{2}} \;\leq\; \Psi^n_j + G(U^n_j, U^n_{j+1})\left(\Phi^n_{j+\frac{1}{2}} - F^n_j\right). \tag{35}$$

Let us denote $G^n_{j+\frac{1}{2}} = G(U^n_j, U^n_{j+1})$ and define the following local numerical dissipation term η^{n+1}_j as

$$\eta^{n+1}_j = S(U^{n+1}_j) - S(U^n_j) + \lambda\left\{G^n_{j-\frac{1}{2}}\,(F^n_j - \Phi^n_{j-\frac{1}{2}}) + G^n_{j+\frac{1}{2}}\,(\Phi^n_{j+\frac{1}{2}} - F^n_j)\right\}. \tag{36}$$

Then,

1. *Such a quantity $\Psi^n_{j+\frac{1}{2}}$ exists;*
2. *Quantity $\Psi(.,.)$ is consistent with the entropy flux, that means that $\Psi(U,U) = \Psi(U)$ for all U in Ω;*

3. The following inequality holds

$$\eta_j^{n+1} \;\geq\; S_j^{n+1} - S_j^n + \lambda\left(\Psi_{j+\frac{1}{2}}^n - \Psi_{j-\frac{1}{2}}^n\right) \quad \forall j \in \mathbb{Z}. \tag{37}$$

Expression (37) defines a numerical entropy flux relative to the numerical flux $\Phi_{j+\frac{1}{2}}^n$.

Proof.

1. Suppose that (34) holds. Then we have

$$\Psi_{j+1}^n - \Psi_j^n \;\leq\; G(U_j^n, U_{j+1}^n)\,\left(F_{j+1}^n - F_j^n\right)$$

or again

$$\Psi_{j+1}^n - G(U_j^n, U_{j+1}^n)\,\left(F_{j+1}^n - \Phi_{j+\frac{1}{2}}^n\right) \;\leq\; \Psi_j^n + G(U_j^n, U_{j+1}^n)\,\left(\Phi_{j+\frac{1}{2}}^n - F_j^n\right),$$

so we can always find a (non unique) $\Psi_{j+\frac{1}{2}}^n$ such that (35) is true.

2. Because G is continuous, the consistency comes from the consistency of the flux $\Phi(.,.)$. Result *3.* is a direct consequence of inequalities (35).

That terminates the proof.

Unfortunately, at the present time, we do not known if it is always possible to build such a vector-valued function $G(U,V)$ for any pair (U,V). For certain states U and V, it is quite easy to build such a G. Indeed, we have first

$$\Psi(V) - \Psi(U) \;=\; \int_0^1 D_U\Psi(U + s(V-U))\,ds\;(V-U).$$

Due to the compatibility relation (3) and to the existence of a Roe matrix linearisation $A(U,V)$ when the system has an entropy-flux pair, we also have

$$\Psi(V) - \Psi(U) \;=\; \int_0^1 D_U S(U + s(V-U))\,D_U F(U + s(V-U))\,ds\;A(U,V)^{-1}\;(F(V) - F(U)).$$

provided that $A(U,V)$ is invertible, so that the vector-valued function X^T, with

$$X \;=\; \int_0^1 D_U S(U + s(V-U))\,D_U F(U + s(V-U))\,ds\;A(U,V)^{-1}$$

is a candidate for $G(U,V)$. It remains to exhibit criteria of consistency. Let us respectively denote

$$\hat{A}(U,V) = \int_0^1 D_U F(U + s(V-U))\,ds, \quad \hat{G}(U,V) = \int_0^1 D_U S(U + s(V-U))\,ds.$$

Then, we can write

$$X - \hat{G}(U,V) = \int_0^1 D_U S(U + s(V-U)) \left[D_U F(U + s(V-U)) - \hat{A}(U,V) \right] ds \; A(U,V)^{-1} + \hat{G}(U,V) \left[\hat{A}(U,V) A(U,V)^{-1} - I \right].$$

Suppose now that, for a given small parameter $\epsilon > 0$, there exists some state $U_0 \in \Omega$ such that $|\lambda_k(A(U_0))| \geq \epsilon$, $\forall k \in \{1, ..., p\}$. By continuity, there exists $\delta > 0$ such that for all $U, V \in \overline{B(U_0, \delta)}$,

$$|\lambda_k(A(U,V))| \geq \epsilon, \; \forall k \in \{1, ..., p\} \text{ and } ||\hat{A}(U,V) A(U,V)^{-1} - I|| \leq \epsilon.$$

Consequently, we have built a candidate for $G(U,V)$ with the above assumptions on U and V.

But the analysis also shows that a difficulty appears when some *"sonic point"* is present in the system. In fact, when a nonlinear discontinuity is stationary, the above construction does not match. This is due to the fact that, in this case, $F(U) = F(V)$ and the jump relations on the entropy give $\Psi(V) - \Psi(U) < 0$ with strict inequality in general.

What we want to emphasize here is that we can wish that the nonconservative dissipation term is a good estimator of a classical discrete entropy inequality at least in cases where there is no stationary waves.

Finally, for implementation purposes and for an easy construction of the convexity dissipation term, it is interesting to consider and analyze the following simple choice for G:

$$G(U,V) = D_U S \left(\frac{U+V}{2} \right).$$

In this case, we prove the following estimate:

Proposition 4 *For any pair $(U,V) \in \Omega^2$ such that $\bar{U} = \frac{U+V}{2} \in \Omega$, there exists a constant $\xi^\star = \xi^\star(U,V) \geq 0$ such that, for any $\xi \geq \xi^\star$,*

$$\left| \Psi(V) - \Psi(U) \; - \; D_U S(\bar{U}) \left(F(V) - F(U) \right) \right| \; \leq \; 2\xi \left[\frac{S(U) + S(V)}{2} - S(\bar{U}) \right]. \tag{38}$$

Proof. We follow some ideas of Harten and Lax [17]. Because it is supposed that the system has an entropy-flux pair, it is hyperbolic ([28]). The structure of the solution of a the Riemann problem of initial states U and V is known. The solution U if self-similar in the space (x,t), that means that we can express $U(x,t)$ as a function $U(s)$, with $s = x/t$. Let us denote by $\xi = \xi^\star(U,V)$, $0 \leq \xi^\star < \infty$ the largest velocity

of propagation (in absolute value). Then, if we denote $\Phi(s;U,V)$ the solution of the Riemann problem parametrized by s, for any $\xi \geq \xi^\star(U,V)$ we have

$$\begin{aligned} F(V) - F(U) &= \int_{-\xi}^{\xi} s \frac{\partial}{\partial s} \Phi(s;U,V)\, ds \\ &= \xi\,(U+V) - \int_{-\xi}^{\xi} \Phi(s;U,V)\, ds \end{aligned}$$

or again

$$\frac{1}{2\xi} \int_{-\xi}^{\xi} \Phi(s;U,V)\, ds \;=\; \frac{U+V}{2} \;-\; \frac{1}{2\xi}\,(F(V) - F(U)) \tag{39}$$

Moreover, because we are looking for an entropy solution of the Riemann problem, the integration of the inequality (4) over the state path of the solution of the Riemann problem gives

$$\begin{aligned} \Psi(V) - \Psi(U) &\leq \int_{-\xi}^{\xi} s \frac{\partial}{\partial \xi} S\left(\Phi(\xi;U,V)\right)\, d\xi \\ &\leq \xi\,(S(U) + S(V)) - \int_{-\xi}^{\xi} S\left(\Phi(s;U,V)\right)\, ds, \end{aligned}$$

or again

$$\frac{1}{2\xi} \int_{-\xi}^{\xi} S\left(\Phi(s;U,V)\right)\, ds \;\leq\; \frac{S(U)+S(V)}{2} \;-\; \frac{1}{2\xi}\,(\Psi(V) - \Psi(U)) \tag{40}$$

Applying the convex function S at each side of equation (39) and applying Jensen inequality gives the inequality

$$S\left(\frac{U+V}{2} \;-\; \frac{1}{2\xi}\,(F(V) - F(U))\right) \;\leq\; \frac{1}{2\xi} \int_{-\xi}^{\xi} S\left(\Phi(s;U,V)\right)\, ds. \tag{41}$$

Using again the convexity of S gives the inequality

$$S\left(\frac{U+V}{2} \;-\; \frac{1}{2\xi}\,(F(V) - F(U))\right) \;\geq\; S\left(\frac{U+V}{2}\right) - \frac{1}{2\xi}\, D_U S\left(\frac{U+V}{2}\right)(F(V) - F(U)). \tag{42}$$

Combining equations (40), (41) and (42) gives a first inequality. Because the states U and V play the same role in this inequality, we also have

$$\Psi(U) - \Psi(V) \;\leq\; D_U S(\bar{U})\,(F(U) - F(V)) + 2\xi \left(\frac{S(U)+S(V)}{2} - S(\bar{U})\right)$$

that gives the inverse inequality and proves (38).

Remark 2 *The inequality*

$$\Psi(V) - \Psi(U) \;-\; D_U S(\bar{U})\,(F(V) - F(U)) \;\leq\; 2\xi \left[\frac{S(U)+S(V)}{2} - S(\bar{U})\right].$$

from (38) is not optimal. Indeed, when U and V are connected by an entropy stationary shock, then $\Psi(V)-\Psi(U)<0$. Below, we give a finer upper bound estimate. But the expression requires the knowledge of the entropy solution $W_R(0;U,V)$ of the Riemann problem of initial left and right states U and V on the characteristic $x/t=0$.

Proposition 5 *Let U and V in Ω such that the entropy solution of the Riemann problem of initial left and right states U and V globally exists. Let us denote $W_R(\xi;U,V)$ this solution on the characteristic $\xi=x/t$. Let us denote by $\Phi^\star=F\left(W_R(0;U,V)\right)$ the Godunov flux of states U and V and $\Psi^\star=\Psi\left(W_R(0;U,V)\right)$ the associated Godunov entropy flux. Then the three following inequalities hold :*

$$\Psi^\star-\Psi(U) \leq D_US(U)\left(\Phi^\star-F(U)\right), \tag{43}$$

$$\Psi(V)-\Psi^\star \leq D_US(V)\left(F(V)-\Phi^\star\right), \tag{44}$$

$$\begin{aligned}\Psi(V)-\Psi(U) \leq\ & D_US(\bar U)\left(F(V)-F(U)\right) \\ & +\left(D_US(V)-D_US(\bar U)\right)\left(F(V)-\Phi^\star\right)+\left(D_US(\bar U)-D_US(U)\right)\left(\Phi^\star-F(U)\right)\end{aligned} \tag{45}$$

for any continuous function $\bar U(U,V)$ such that $\bar U(U,U)=U$.

4 Application to the construction of a conservative hybrid scheme

Usual hybrid schemes compute hybrid fluxes between second order scheme (like Lax Wendroff) and first order schemes (like Lax-Friedrichs). The flux combination coefficients $\theta^n_{j+\frac12}$, $0\leq\theta^n_{j+\frac12}\leq1$ are usually designed in such a way that they preserve the second order accuracy in smooth regions of the solution whereas they "switch" to the first order order scheme near lines of discontinuity in order to be stable (see for example [4], [20] and [44]). Classical strategies of switch function are based on limiters of flux using classical limiter functions (*minmod*, ...). Halaoua [16] for example has tested some hybrid schemes for the resolution of two-phase flow problems.

We here propose to build an hybrid conservative scheme that takes advantage of the previous convexity dissipation estimate for computing the combination coefficients $\theta^n_{j+\frac12}$. We propose to hybridize the Modified Lax-Friedrichs flux Φ^{MLF} and the approximate Lax-Wendroff flux $\Phi^{LW,\epsilon}$ as follows:

1. First, compute local values of θ_j^n centered on each cell j using the local convexity dissipation term. We propose the following construction: find the smallest value $\theta_j^n = \theta_j^n\left(S, \lambda, U_{j-1}^n, U_j^n; U_{j+1}^n\right)$ in $[0,1]$ that solves the inequation $\eta_j^{n+1}(\theta_j^n; S, \lambda, U_{j-1}^n, U_j^n; U_{j+1}^n) \leq 0$. For an easy implementation, we can proceed as follows:

   Algorithm. - Let $\Delta\theta_j^n > 0$ be a small increment. We build the sequences $(\theta_j^{n,q})_{q\in\mathbb{N}}$ as follows: let $q = 0$, $\theta_j^{n,0} = 0$.

$$
\begin{array}{l}
\textbf{while } \left(\left(\eta_j^{n+1}(\theta_j^{n,q}) > \delta\right) \textbf{ and } \left(\theta_j^{n,q} \leq 1\right)\right) \textbf{do} \\
\quad \theta_j^{n,\,q+1} \;=\; \theta_j^{n,q} \;+\; \Delta\theta_j^n; \\
\quad q \;=\; q+1; \\
\quad \textbf{compute } \eta_j^{n+1}(\theta_j^{n,q}); \\
\textbf{end while} \\
\textbf{set } \theta_j^n \;=\; \theta_j^{n,q}.
\end{array}
\tag{46}
$$

2. Then compute the hybrid numerical flux as follows

$$
\begin{aligned}
\theta_{j+\frac{1}{2}}^n &= \max(\theta_j^n, \theta_{j+1}^n), \\
\Phi_{j+\frac{1}{2}}^n(\theta_{j+\frac{1}{2}}^n; U_j^n, U_{j+1}^n, \lambda) &= \theta_{j+\frac{1}{2}}^n\, \Phi_{j+\frac{1}{2}}^{MLF}(U_j^n, U_{j+1}^n, \lambda) \;+\; (1-\theta_{j+\frac{1}{2}}^n)\, \Phi_{j+\frac{1}{2}}^{LW,\epsilon}(U_j^n, U_{j+1}^n, \lambda).
\end{aligned}
$$

Proceeding like that, we obtain a conservative scheme which only require flux evaluations, with no derivative or Jacobian matrix computations. However, each numerical flux needs an iterative method to solve the inequation $\eta_j^{n+1}(\theta_j^n; S, \lambda, U_{j-1}^n, U_j^n; U_{j+1}^n) \leq 0$. Of course, one could use Newton's method to reduce the number of iterations.

5 Extension of the method to systems with nonconservative products and nonhomogeneous source terms

Although this is not the objectives of the present paper, we would like to emphasize that is also possible to extend this method when nonconservative terms and source terms are present in the system. This is necessary if we want to use this method in the framework of multiphase flows where mass, momentum

and energy transfers between phases make appear such terms.

In this paper, we will restrict ourselves to a short analysis to give one the flavour of the additional difficulties.

We now consider the following system of first order partial differential equations

$$\partial_t U \ + \ \partial_x F(U) \ + \ B(U)\partial_x U \ = \ T(U),$$

where $B(U)\partial_x U$ is the nonconservative term and $T(U)$ is the source term.

5.1 Source terms

As first step, let us show that that the source term alone introduces new difficulties. Imagine we want to solve the following second order system:

$$\partial_t U^\epsilon \ = \ T(U^\epsilon) \ + \ \epsilon\, \partial_x (\mathcal{D}(U^\epsilon)\partial_x U^\epsilon)$$

for a small parameter $\epsilon > 0$ and for a positive viscosity matrix $\mathcal{D}(.)$ (positive in the sense of a particular metrics). Multiplying par $D_U S(U)$ gives

$$\partial_t S(U^\epsilon) \ = \ D_U S(U^\epsilon)\, T(U^\epsilon) \ + \ \epsilon\, \partial_x \left(D_U S(U^\epsilon)\, \mathcal{D}(U^\epsilon)\partial_x U^\epsilon \right) \ - \ \epsilon \left(D^2_{UU} S(U^\epsilon)\, \mathcal{D}(U^\epsilon)\partial_x U^\epsilon, \partial_x U^\epsilon \right). \quad (47)$$

We would like to pass to the limit when ϵ vanishes. Under classical hypotheses (L^1 convergence of U^ϵ to U, uniform L^∞ bounds on U^ϵ) and if $\left(D^2_{UU} S(U)\, \mathcal{D}(U^\epsilon)\xi, \xi \right) > 0$ for $\xi \neq 0$, it can be shown that U verifies the following system of equations

$$\partial_t U \ = \ T(U), \ x \in \mathbb{R}, t > 0, \quad (48)$$

and

$$\partial_t S(U) \ - \ D_U S(U) T(U) \ \leq \ 0, \ x \in \mathbb{R}, t > 0, \quad (49)$$

in the sense of distributions $\mathcal{D}'(\mathbb{R} \times \mathbb{R}^+)$. In fact, it is easy to see that the second term of the right hand side of (47) tends to zero whereas the last term stays negative. One can ask the question if it is easy to preserve inequality (49) at the discrete level. The forward Euler discretization of (48) at point x_j gives

$$U_j^{n+1} \ = \ U_j^n \ + \ \tau^n T_j^n,$$

with $T_j^n = T(U_j^n)$ and τ^n is the time step. A candidate for a (so-called) dissipation term would be

$$\eta_j^{n+1} \;=\; S_j^{n+1} - S_j^n \;-\; \tau^n D_U S_j^n \, T_j^n, \tag{50}$$

where $D_U S_j^n = D_U S(U_j^n)$. Unfortunately, the exact second order Taylor expansion under integral form

$$S_j^{n+1} \;=\; S_j^n + D_U S_j^n \left(U_j^{n+1} - U_j^n\right) \;+\; \int_0^1 (1-t) D_{UU}^2 S(U_j^j + t(U_j^{n+1} - U_j^n))\, dt \;\left(U_j^{n+1} - U_j^n, U_j^{n+1} - U_j^n\right)$$

shows that

$$\eta_j^{n+1} \;\geq\; 0$$

for a strictly convex function S, so that η_j^{n+1} has the bad sign. In order to retrieve the good sign, we should rather consider the following dissipation term:

$$\eta_j^{n+1} \;\stackrel{\text{def}}{=}\; S_j^{n+1} - S_j^n \;-\; \tau^n D_U S_j^{n+1} \, T_j^n$$

By same arguments, we get

$$S_j^{n+1} - S_j^n - D_U S_j^{n+1} \left(U_j^{n+1} - U_j^n\right) \;=\; -\int_0^1 (1-t) D_{UU}^2 S(U_j^{n+1} + t(U_j^n - U_j^n + 1))\, dt \;\left(U_j^{n+1} - U_j^n, U_j^{n+1} - U_j^n\right)$$

and

$$U_j^{n+1} - U_j^n \;=\; \tau^n T_j^n$$

so that

$$\eta_j^{n+1} \;\leq\; 0.$$

Remark that this estimate is unconditional with respect to the time step τ^n.

5.2 Nonconservative products

We now deal with the following system

$$\partial_t U \;+\; \partial_x F(U) \;+\; B(U) \partial_x U \;=\; 0. \tag{51}$$

In hyperbolic systems,the question of the correct discretization of nonconservative products is still an open problem. Although some negative results have been concluded for nonconservative schemes (Hou and Le Floch [19]), we need to face such systems because lots of models lead to such kind of equations, especially in the case of multiphase flows. We would like to propose natural extensions of the Modified

Lax-Friedrichs and the Lax-Wendroff scheme when a nonconservative product is present.

We assume that all the information on wave propagation in the system is included in the flux term F, whereas the product $B(U)\partial_x U$ expresses exchange phenomena (transfers between phases for example). For the models we are interested in, we will have $\sum_{k\in\mathcal{S}_j}\left(B(U)\partial_x U\right)_k = 0$ for some sets $\mathcal{S}_j \subset \{1,...,p\}$, that means that some mean quantities are conserved.

First, because the Modified Lax-Friedrichs scheme is based on the integration of the exact solution on the domain $]x_{j-1}, x_{j+1}[\times]t^n, t^{n+1}[$, one can propose

$$U_j^{n+1} = U_j^n - \lambda^n \left(\Phi_{j+\frac{1}{2}}^{MLF,n} - \Phi_{j-\frac{1}{2}}^{MLF,n}\right) - \frac{\lambda}{2}\left(B_{j-\frac{1}{2}}^n (U_j^n - U_{j-1}^n) + B_{j+\frac{1}{2}}^n (U_{j+1}^n - U_j^n)\right), \qquad (52)$$

where the $B_{j+\frac{1}{2}}^n$ are some mean matrices, for example

$$B_{j+\frac{1}{2}}^n \;=\; B\left(\frac{U_j^n + U_{j+1}^n}{2}\right).$$

For the Lax-Wendroff scheme, the basic Lax-Wendroff flux $\Phi_{j+\frac{1}{2}}^n$ can be interpreted as the integration of the physical flux, solution of

$$\partial_t F(U) \;+\; A(U)\partial_x F(U) \;=\; 0$$

(for smooth solutions) on the domain $]x_j, x_{j+1}[\times]t^n, t^n + \frac{1}{2}\tau^n[$. Taking now into account the nonconservative product, we first remark that, for smooth solutions, the physical flux is solution of

$$\partial_t F(U) \;+\; A(U)\partial_x F(U) \;+\; A(U)\,B(U)\partial_x U \;=\; 0.$$

That leads to a Lax-Wendroff flux enriched by the nonconservative term:

$$\Phi_{j+\frac{1}{2}}^{LW,n} \;=\; \frac{1}{2}\left(F_j^n + F_{j+1}^n\right) - \frac{\lambda}{2}\left(A_{j+\frac{1}{2}}^n \left(F_{j+1}^n - F_j^n\right) + A_{j+\frac{1}{2}}^n B_{j+\frac{1}{2}}^n \left(U_{j+1}^n - U_j^n\right)\right). \qquad (53)$$

Again, because we do not want to compute any derivative in our method, we replace it by an approximate Lax-Wendroff flux $\Phi_{j+\frac{1}{2}}^{LW,\epsilon}$ where the terms $A_{j+\frac{1}{2}}^n \left(F_{j+1}^n - F_j^n\right)$ and $A_{j+\frac{1}{2}}^n B_{j+\frac{1}{2}}^n \left(U_{j+1}^n - U_j^n\right)$ are approximated by numerical directional derivatives using a small real parameter ϵ:

$$\begin{aligned}
A_{j+\frac{1}{2}}^n \left(F_{j+1}^n - F_j^n\right) &\approx \frac{1}{\epsilon}\left(F(U_{j+\frac{1}{2}}^n + \epsilon\left(F_{j+1}^n - F_j^n\right)) - F(U_{j+\frac{1}{2}}^n)\right), \\
A_{j+\frac{1}{2}}^n B_{j+\frac{1}{2}}^n (U_{j+1}^n - U_j^n) &\approx \frac{1}{\epsilon}\left(F(U_{j+\frac{1}{2}}^n + \epsilon\, B_{j+\frac{1}{2}}^n \left(U_{j+1}^n - U_j^n\right)) - F(U_{j+\frac{1}{2}}^n)\right)
\end{aligned}$$

Then the approximate Lax-Wendroff scheme becomes

$$U_j^{n+1} = U_j^n - \lambda \left(\Phi_{j+\frac{1}{2}}^{LW,\epsilon,n} - \Phi_{j-\frac{1}{2}}^{LW,\epsilon,n} \right) - \frac{\lambda}{2} \left(B_{j-\frac{1}{2}}^n (U_j^n - U_{j-1}^n) + B_{j+\frac{1}{2}}^n (U_{j+1}^n - U_j^n) \right), \tag{54}$$

with

$$\Phi_{j+\frac{1}{2}}^{LW,\epsilon,n} = \frac{F_j^n + F_{j+1}^n}{2} - \frac{\lambda}{2\epsilon} \left(F(U_{j+\frac{1}{2}}^n + \epsilon\,(F_{j+1}^n - F_j^n)) - F(U_{j+\frac{1}{2}}^n) + F(U_{j+\frac{1}{2}}^n + \epsilon\, B_{j+\frac{1}{2}}^n\,(U_{j+1}^n - U_j^n)) - F(U_{j+\frac{1}{2}}^n) \right).$$

Consequently, the hybrid scheme in this context is

$$U_j^{n+1} = U_j^n - \lambda \left(\Phi_{j+\frac{1}{2}}^n - \Phi_{j-\frac{1}{2}}^n \right) - \frac{\lambda}{2} \left(B_{j-\frac{1}{2}}^n (U_j^n - U_{j-1}^n) + B_{j+\frac{1}{2}}^n (U_{j+1}^n - U_j^n) \right), \tag{55}$$

with

$$\Phi_{j+\frac{1}{2}}^n = \theta_{j+\frac{1}{2}}^n\, \Phi_{j+\frac{1}{2}}^{MLF} + (1 - \theta_{j+\frac{1}{2}}^n)\, \Phi_{j+\frac{1}{2}}^{LW,\epsilon,n}.$$

6 Numerical experiments

For numerical experiments, we investigate numerical solutions of scalar problems with pure advection equation and Burgers equation, the Sod shock tube problem for the 1D system of Gas Dynamics, a slow moving contact discontinuity, a transonic rarefaction fan, a stationary supersonic-subsonic 1D nozzle flow, the Collela and Woodward interacting blast wave problem, a pure compressible water shock tube problem, a test case with nonsmooth and tabulated equations of state, the well-known two-phase flow faucet problem proposed by Ransom [37], and finally a two-dimensional problem of shock reflection on a wall for the Euler equations.

6.1 Numerical study of the approximation error for the linear advection equation

The accuracy of the method in terms of the values of the parameter θ is formal. We have performed a numerical study of the linear advection equation with a smooth initial data in order to evaluate both accuracy and degree of degeneracy of the accuracy at local extrema. For that, we consider the following

scalar problem

$$\partial_t u \ + \ \partial_x u \ = \ 0, \ x \in]0,1[, t > 0,$$

$$u(x,0) \ = \ \sin(\pi x + \pi/4), \ x \in]0,1[,$$

$$u(0,t) \ = \ \sin(-\pi t + \pi/4), \ t > 0.$$

The analytic solution of that problem is clearly

$$u(x,t) \ = \ \sin\left(\pi(x-t) + \pi/4\right).$$

We experiment our hybrid scheme on that problem using a uniform mesh made of 400 points and a CFL number equal to 0.5. As convex function $s(u)$, we use

$$s(u) \ = \ u \, \log(1+u).$$

At final time $T = t^N = 0.375$, we respectively show the profiles of the discrete solution, the corresponding profiles of θ coefficients and function η and the $\log_{10}$-relative error profile ϵ_j^N at each computational point:

$$\epsilon_j^N = \log_{10} \left| u_j^N - u(x_j, t^N) \right|.$$

We also compare this error with the one obtained using the pure Lax-Wendroff scheme (see figure 3). The function η stays negative as expected. We observe that the parameter θ is "activated" in certain regions of the solution according to the sign of the first and second derivatives of u. The parameter θ is particularly more strongly activated in the right vicinity of the extremum of the solution, making the scheme first order accurate in that region. The error near the extremum is dispersed during time iterations. On the extreme right part of the computational domain, the function θ is activated but stays quite small (of the order of 10^{-2}). The error of approximation is almost of the order of that obtained by the Lax-Wendroff scheme.

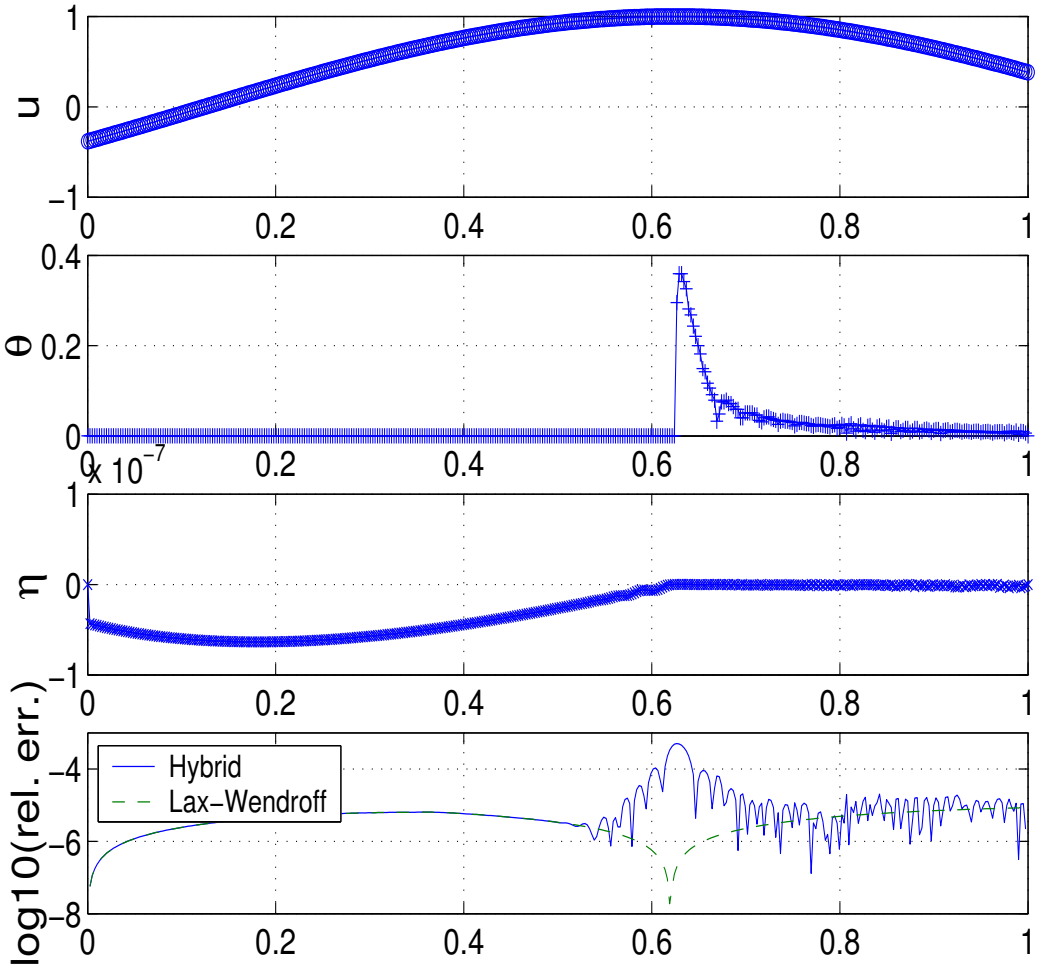

Figure 3: Experimental error study for the advection equation and a smooth initial data. Comparison of the error with the pure Lax-Wendroff scheme.

6.2 The Burgers equation

In this section we are looking for solutions of the scalar problem with the one-dimensional inviscid Burgers equation:

$$\partial_t u + \partial_x(u^2/2) = 0,\ x \in]0,1[,\ t > 0, \tag{56}$$

$$u(x,0) = u^0(x), \tag{57}$$

for some given initial data $u^0 \in L^\infty(0,1) \cap BV(0,1)$. Because the equation is scalar, it admits lots of entropy pairs. Indeed, any convex function $s(u)$ is an entropy with associated entropy flux $\psi(u) = \int_u v s'(v)\, dv$.

In order to understand how the scheme behaves on simple compression waves, rarefaction fans and shock waves, we propose to follow the evolution of the solution of initial data:

$$u^0(x) = \begin{cases} 0 & \text{for } 0 \le x < 0.2, \\ 1 & \text{for } 0.2 \le x < 0.4, \\ 1 - 5(x - 0.4) & \text{for } 0.4 \le x < 0.6, \\ 0 & \text{otherwise.} \end{cases} \tag{58}$$

The initial discontinuity must degenerate into a rarefaction fan whereas the compression zone between $x = 0.4$ and $x = 0.6$ must sharpen itself to produce a shock wave that propagates from $x = 0.6$ at velocity $\sigma = 0.5$. For larger times, rarefaction and shock wave interact. As we can see on figure 6.6, the numerical solution is quite stable during time evolution and accurate. The combination coefficients $\theta^n_{j+\frac{1}{2}}$ are close to zero in the regions of smoothness. That means that the scheme almost has the accuracy of a second order scheme. In the other hand, θ raises up to 1 through the shock wave.s Remark that the strongest activation of θ is located behind the shock wave. That means that infinitesimal oscillations generated by the discontinuity are rapidly killed by the sufficient rate of numerical dissipation.

6.3 Sod shock tube problem for the compressible Euler equations

We are now dealing with the well-known one-dimensional compressible Euler equations with the hypothesis of perfect diatomic polytropic gas,

$$\partial_t U + \partial_x F(U) = 0,\ x \in]0,1[,\ t > 0, \tag{59}$$

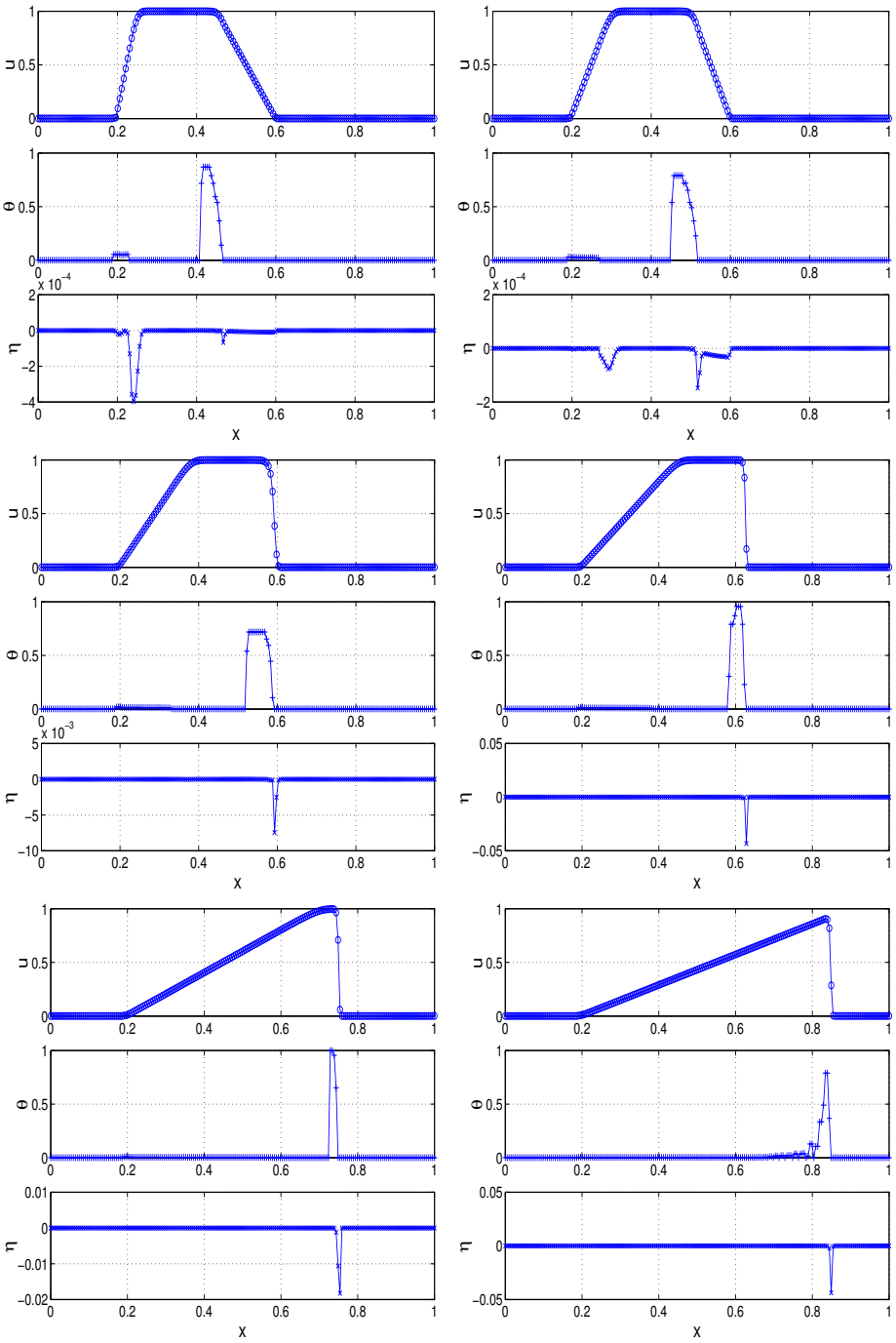

Figure 4: Burger's equation: rarefaction fan-shock interaction problem. Numerical solutions at different times with a uniform mesh made of 200 points, CFL=0.5: $T = 0.05s$, $T = 0.1s$, $T = 0.18s$, $T = 0.25s$, $T = 0.5s$ and $T = 0.7s$. At each time, profiles of discrete solution, θ and numerical dissipation η are plotted.

where $U = (\rho, \rho u, \rho E)$, $F(U) = (\rho u, \rho u^2 + p, (\rho E + p)u)$, variable ρ is the density of fluid, u the velocity, p the pressure, ρE the volumic energy and the equation of state is

$$p = (\gamma - 1)\left(\rho E - \frac{1}{2}\rho u^2\right), \ \gamma = 1.4\,.$$

The Sod shock tube problem [42] consists in a piecewise constant initial data made of two constant left and right states $U_L = (\rho_l, \rho_l u_l, \rho_l E_l)$ and $U_R = (\rho_r, \rho_r u_r, \rho_r E_r)$ with an interface at $x = 0.5$. This corresponds to a Riemann problem. The exact solution is made of a 1-rarefaction, a 2-contact discontinuity and a 3-shock. Initial values are the following:

Left state	Right state
$\rho_l = 1$	$\rho_r = 0.125,$
$u_l = 0$	$u_r = 0,$
$p_l = 1$	$p_r = 0.1\,.$

Even though entropy pairs are known for this system, for example $S(U) = -\rho \log(p/\rho^\gamma)$, $\Psi(U) = u\,S(U)$, we deliberately use the simplest convex function $\tilde{S}(U) = \frac{1}{2}||U||_2{}^2$ (which has no entropy flux) in the numerical method to demonstrate that stability is performed with this choice. We obtain satisfactory results. Although our scheme is only first order accurate, the numerical rarefaction fan is accurately captured and the quality is not so far from that obtained by usual second order schemes. One can remark that, in smooth region, coefficient θ does not exceed 0.025 so that the resulting numerical flux is very close to Lax-Wendroff one. Using a CFL number equal to 0.5, the shock wave is captured on 4 or 5 points. No oscillation appears at the "eye norm". Unfortunately, the level of accuracy for the capture of the contact wave is not so good. In this region, results are comparable to those obtained by first order Godunov-type schemes. We observe that, through the 2-wave, coefficient θ adapts itself around a mean value of order 0.2.

Another observation is that the space profile of θ is not smooth. What we plot is the value of all the θ_j but recall that the real coefficient used in the scheme is $\theta^n_{j+\frac{1}{2}} = \max(\theta^n_j, \theta^n_{j+1})$. Anyway, the profile of the $\theta_{j+\frac{1}{2}}$ is not also smooth, that means that the numerical fluxes are not smooth! Although the classical analysis of convergence of conservative scheme requires smoothness of the numerical fluxes (at least Lipschitz continuous), the behaviour of our numerical scheme is quite good. We also performed computations on finer space grids and did not point out any problem.

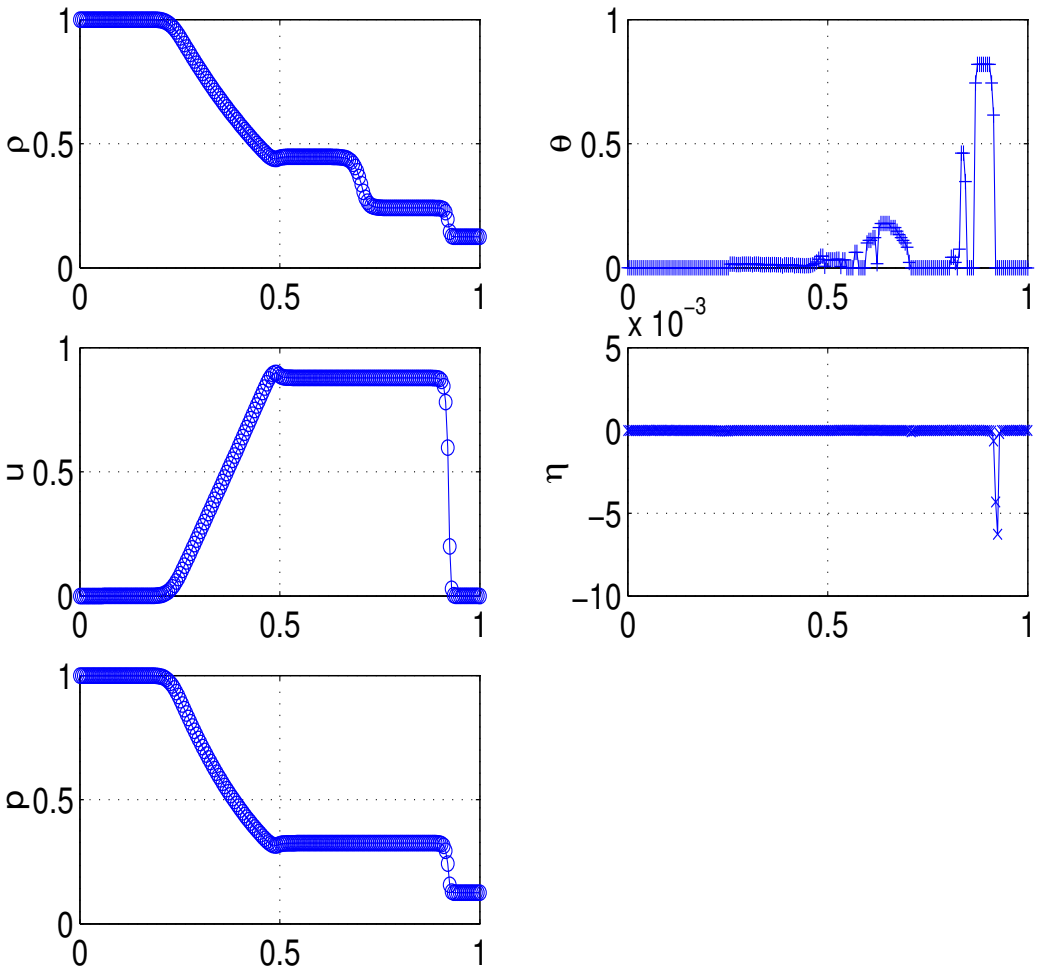

Figure 5: Sod shock tube problem, uniform mesh, 200 points, CFL=0.5. Numerical solution, $T = 0.23$.

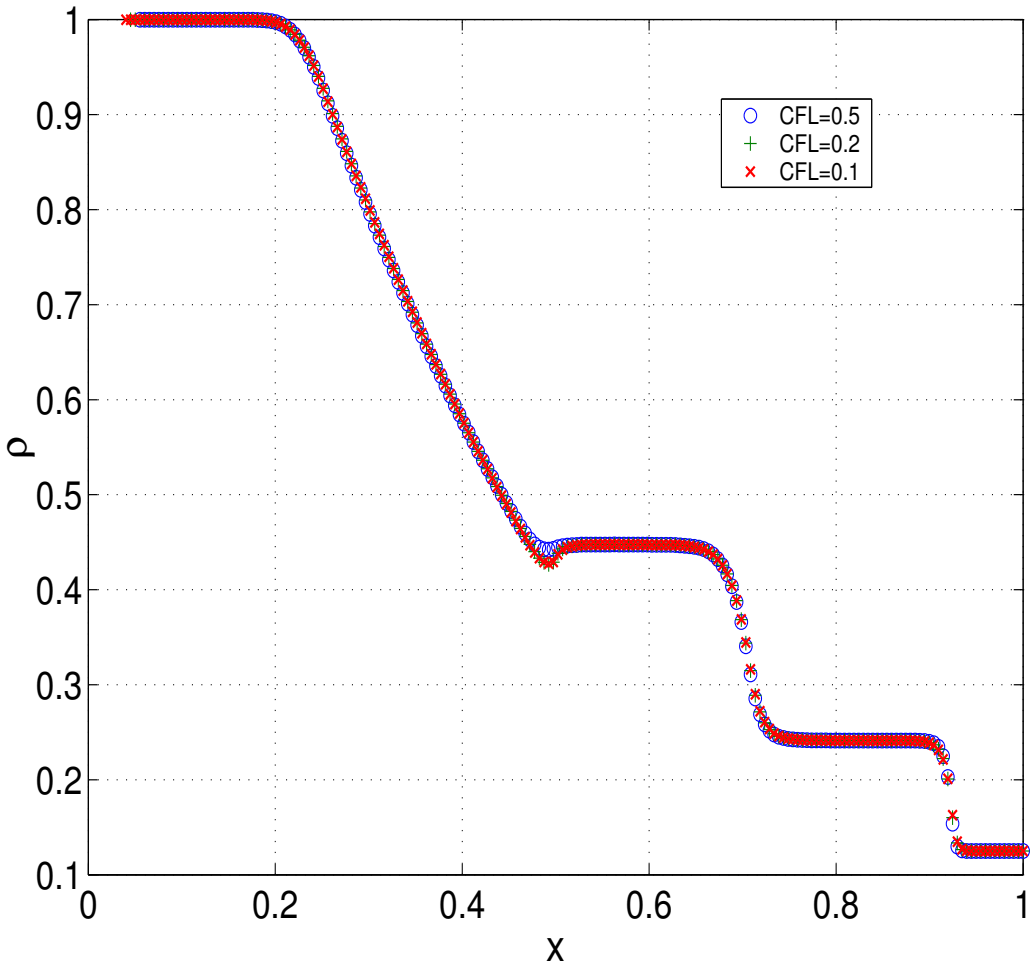

Figure 6: Influence of the CFL number, density profile, 200 points for CFL=0.5 (o), 0.2 (+) and 0.1 (x)

We have also tested the influence of the choice of the CFL number on the numerical dissipation of the scheme. On figure 6, three computations are done with different constant values of the CFL number, respectively 0.5, 0.2 and 0.1. We do not see big differences on the density profiles, except a small undershoot at the corner of the rarefaction fan that appears using CFL= 0.2 and 0.1. The rate of numerical dissipation is of the same order for the three results.

6.4 A low speed contact discontinuity for the Euler equations

This test case is presented in In [24]. The aim of this test is to investigate the accuracy of the proposed scheme, actually its numerical dissipation, inside a slowly moving contact discontinuity. The initial conditions for this test are

Left state	Right state
$\rho_l = 1$	$\rho_r = 0.1,$
$u_l = 0.5$	$u_r = 0.5,$
$p_l = 10^5$	$p_r = 10^5\,.$

We use a uniform grid with 100 mesh points and a CFL number equal to 0.5. On figure 7, we present the density profile at final time $T = 6\,10^{-4}$ s with corresponding θ and dissipation rate profiles. What we see it that the numerical dissipation is very small through the low-moving contact discontinuity. A comparison of this result with those presented in In [24] shows that, although our scheme is a central-like scheme, the quality of capture is of the order of Godunov-type schemes (and relaxed versions of them). In particular, the scheme gives far better results than the HLLE (for Harten, Lax, van Leer and Einfeld) scheme and flux vector splitting schemes in this case. This test case let us think that this method is adapted to the computation of stationary problems for which the capture of contacts is critical (high Reynolds number problems, multi-material, multiphase problems).

Let us however mention the existence of instabilities on the profile of parameter θ that arbitrary evolves through regions of quasi-constant states but do not produce spurious oscillations on the variables of interest.

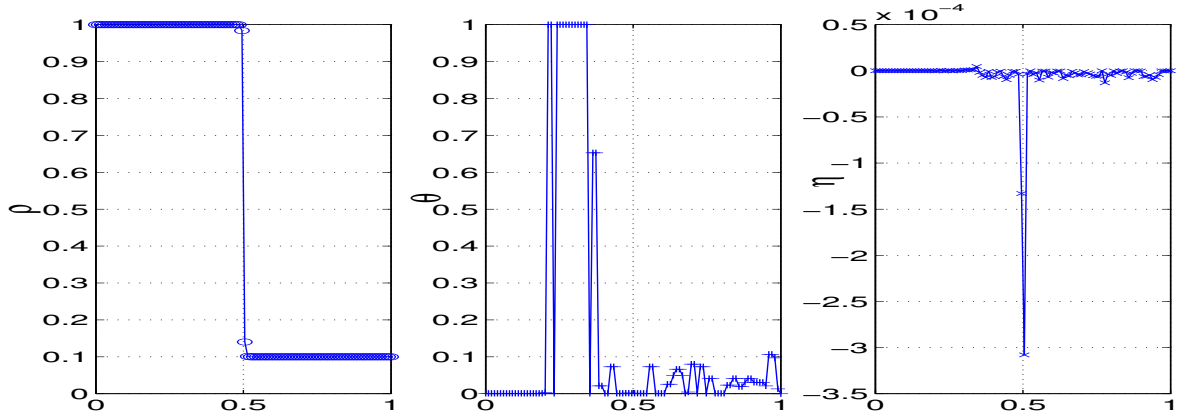

Figure 7: Sod shock tube problem, uniform mesh, 200 points, CFL=0.5. Numerical solution, $T = 0.23$.

6.5 Transonic rarefaction fan

As already remarked in section 3.1, the criterion defined by the local nonconservative dissipation term (22) is weaker than the usual entropy condition. In particular, an entropy-violating stationary shock for conservative equations can satisfy the nonconservative criterion. We would like to illustrate this behaviour numerically. Let us consider again the classical gas Dynamics system and the shock tube problem of initial data

Left state	Right state
$\rho_l = 5$	$\rho_r = 0.125,$
$u_l = 0$	$u_r = 0,$
$p_l = 5$	$p_r = 0.1\,.$

The structure of the solution of the Riemann problem contains a transonic 1-rarefaction fan. It is well-known that entropy-violating schemes generally capture a nonentropic expansion shock inside the sonic fan. Figure 8 indeed shows that the hybrid scheme violates the entropy condition and the condition η_j^{n+1} does not introduce enough numerical dissipation at the sonic point.

This feature is the major drawback of the method and can seem to be a major flaw. But let us first remark that numerous entropy-violating numerical schemes like Roe [39] and variant methods [21], flux schemes [22], [10] today are still intensively used for complex fluid flows.

On the over hand, recents work of Coquel and Perthame [12] and In [24] have shown that the relaxation technique can be used as a universal entropy fix for general entropy-violating schemes. Of course, we can

define a relaxed version of our hybrid scheme; let us briefly present its construction (see the reference article [12] for more details): the equation of state

$$e = \frac{1}{\gamma - 1}\frac{p}{\rho},\ \gamma = 1.4,$$

is splitted up into two internal energies $e = e_1 + e_2$ with

$$e_1(p, \rho) = \frac{1}{\gamma_1 - 1}\frac{p}{\rho}.$$

The subcharacteristic condition given by Coquel-Perthame [12] requires to use a constant γ_1 greater than γ. In the evolution step of the procedure, the initial system

$$\partial_t U + \partial_x F(U) = 0,$$

where $U = (\rho, \rho u, \rho E)^T$, $E = \frac{1}{2}\rho u^2 + \rho e$, is replaced by the four-equation system

$$\partial_t W + \partial_x \tilde{F}(W) = 0, \tag{60}$$

where

$$W = (\rho, \rho u, \rho E_1, \rho e_2)^T,\ \tilde{F}(W) = \big(\rho u, \rho u^2 + p_1, (\rho E_1 + p_1)u, \rho e_2 u\big)^T,\ E_1 = \frac{1}{2}u^2 + e_1(\rho, p_1)$$

Remark that the part e_2 of the internal energy is simply convected at the velocity u. In the relaxation step at instantaneous equilibrium, we expect to have the pressure equilibrium

$$p = p(\rho, e) = p_1(\rho, e_1).$$

or again

$$e = \frac{1}{\gamma - 1}\frac{p}{\rho},\ e_1 = \frac{1}{\gamma_1 - 1}\frac{p}{\rho}. \tag{61}$$

At the computational point of view, a new field of internal energy $(e_2)_j^n$ is computed at each time step before the evolution in time according to (61) and $e_2 = e(\rho, p) - e_1(\rho, p)$ (relaxation step of the procedure with instantaneous equilibrium). The resulting relaxed hybrid scheme consists in two steps:

1. first, apply the hybrid scheme to the system (60) and compute numerical fluxes $\tilde{\Phi}^n_{j+\frac{1}{2}}$ (with four components) at each interface $j + \frac{1}{2}$. Left us denote by $\Phi^n_{j+\frac{1}{2};123}$ the vector made of the three first components of vector $\tilde{\Phi}^n_{j+\frac{1}{2}}$ and $\Phi^n_{j+\frac{1}{2};4}$ its fourth component.

2. secondly, compute the final numerical flux, consistent with the original three-components flux F by the following construction:

$$\Phi^n_{j+\frac{1}{2}} \;=\; \Phi^n_{j+\frac{1}{2};123} + \left(0, 0, \Phi^n_{j+\frac{1}{2};4}\right)^T.$$

We have performed a numerical simulation with the following parameters: $\gamma = 1.4$, $\gamma_1 = 3$, $S(W) = \frac{1}{2}||W||^2$, $CFL = 0.45$, $T = 0.18$, 100 mesh points. We can see on figure 9 that the relaxation procedure indeed provides the entropy property. To conclude here, the relaxation technique is a very good alternative for providing the full entropy property to our numerical scheme. On the over hand, it makes the relaxed hybrid method a little bit less easy and direct to implement because we need to study the equations of states.

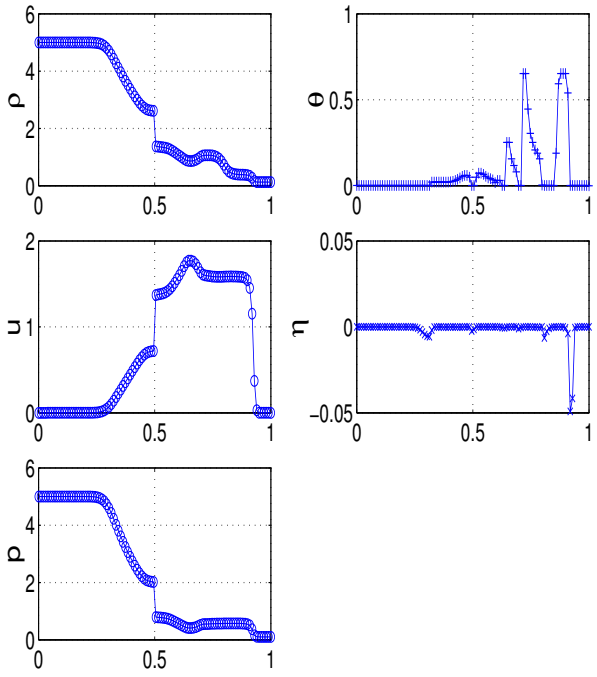

Figure 8: Transonic rarefaction fan problem, uniform mesh, 100 points, CFL=0.45. Numerical solution at final time $T = 0.18$. An expansion shock appears.

6.6 Steady-state computation into a nozzle for the 1D Euler equations

We are now looking for the steady state of a flow into a nozzle with supersonic inflow and subsonic outflow. This involves a stationary shock wave within the flow. We use a one-dimensional model and

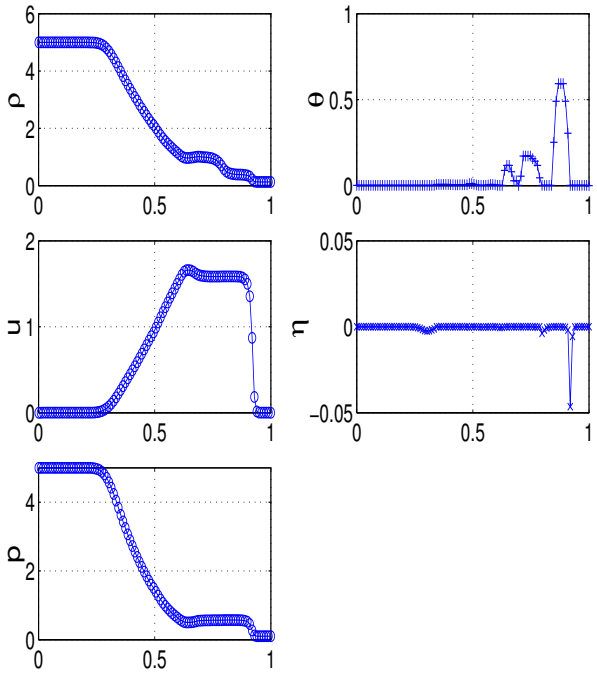

Figure 9: Transonic rarefaction problem. Numerical solution using a relaxed version of the hybrid scheme

the Euler equations with the presence of a space-varying cross-section. This test case is standard and is presented *e.g.* in [8].

Suppose that the area of the cross-section is

$$a(x) = 1.398 + 0.347 \, \tanh(0.8\, x + 0.4)$$

for $0 \leq x \leq 10$. The Euler equations in the nozzle are

$$\begin{aligned} (a\rho)_t + (a\rho u)_x &= 0, \\ (a\rho u)_t + (a(\rho u^2 + p))_x &= p\, a'(x), \\ (a\rho E)_t + (a(\rho E + p)u)_x &= 0, \end{aligned}$$

where

$$\begin{aligned} E &= e + u^2/2, \\ p &= (\gamma - 1)\rho e, \ \gamma = 1.4. \end{aligned}$$

When the steady state is reached, the boundary data are

$$\rho(0) = 0.5, \qquad \rho(10) = 0.741284,$$
$$u(0) = 1.41986, \quad u(10) = 0.577022,$$
$$p(0) = 0.5, \qquad p(10) = 0.919514.$$

There is an upstream supersonic state to the left with Mach number $M_\infty = 1.2$ and a downstream state to the right with $M = 0.438$. All three variables in the numerical solution are specified at the supersonic inflow boundary. At the subsonic outflow boundary, the outflow data given above are used to specify the characteristic variable corresponding to the characteristic going to the left. For the initialization, the initial solution is obtained by linear interpolation on the conservative variables between the left and the right state. On figure 10 we represent the numerical solution whereas on figure 11, it is plotted two different convergence histories to the steady state. We used a space 80 points uniform grid. We see

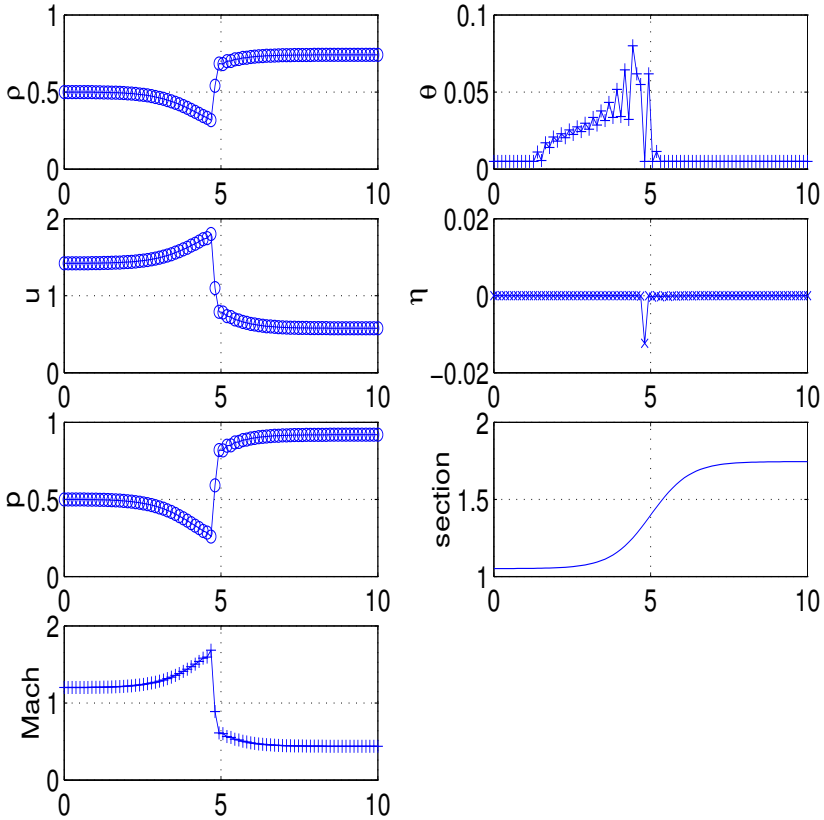

Figure 10: Steady state into a supersonic-subsonic nozzle flow.

that the numerical solution is very accurate. The stationary shock is spread out over one point. We have

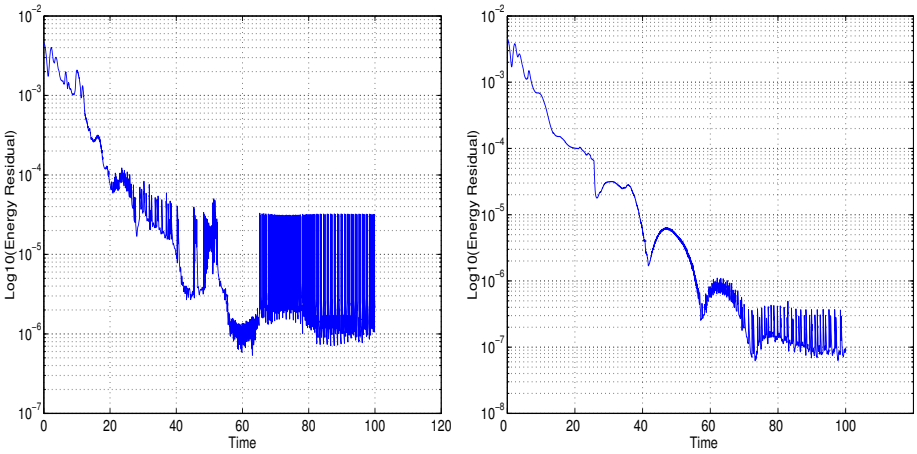

Figure 11: Steady state into a supersonic-subsonic nozzle flow. Convergence history to the steady state. The difficulties of convergence are due to the inaccurate incremental process of the evolution of θ within the algorithm. The second history corresponds to a finer incremental process of computation of θ for η_j^{n+1}.

slightly changed the algorithm for the computation of θ_j^n and have taken advantage of the convergence to a steady state in order to accelerate the computation. We keep in memory the value of θ_j^{n-1}, decrement it to a certain value $\Delta\theta_j^{n-1} > 0$ and use $(\theta_j^{n-1} - \Delta\theta_j^{n-1})$ as initial value of the fixed algorithm instead of 0 for the solution of the inequation $\eta_j^{n+1}(\theta_j^n) \leq 0$. It is clear that this initialization involves very few iterations compared to the original algorithm.

On figure 11, we want to emphasize that the level of accuracy to solve the inequation $\eta_j^{n+1}(\theta_j^n) \leq 0$ in the sense of the algorithm explained in a previous section can have a strong influence on the convergence rate to the steady state. Once we find the index k such that $\theta_j^{n,k} = \theta_j^{n,k-1} + \Delta\theta_j^{n,k-1} < \delta$ for a very small fixed parameter δ, we use $\theta_j^n = \theta_j^{n,k}$ as final value. Of course, it depends on the value $\Delta\theta_j^{n,k-1}$. On this computation, it is observed that the steady state is "reached" faster when smaller increments $\Delta\theta_j^{n,k-1}$ are used. Otherwise, some noise persists in the field of θ that only allows for decreasing to a few orders of magnitude of the residual.

6.7 Woodward and Collela interacting blast waves problem

This is a well-known difficult problem where the numerical solution is very sensitive to the numerical dissipation of the scheme. A systematic comparison of numerical results using state-of-the-art numerical scheme on this problem can be found in Liska and Wendroff [30]. The classic Woodward-Collela blast wave problem [43] computes the interaction of waves from two Riemann problems for the compressible Euler equations (59) with reflecting boundary conditions. The problem is treated again on the interval $x \in (0, 1)$. Two initial discontinuities are located at $x_1 = 0.1$ and $x_2 = 0.9$. The initial density is one and the velocity is zero everywhere. Initial pressures in three different regions (left p_l, middle p_m and right p_r) are $(p_l; p_m; p_r) = (1000; 0.01; 100)$. We use a uniform grid made of 2000 cells. In order to obtain

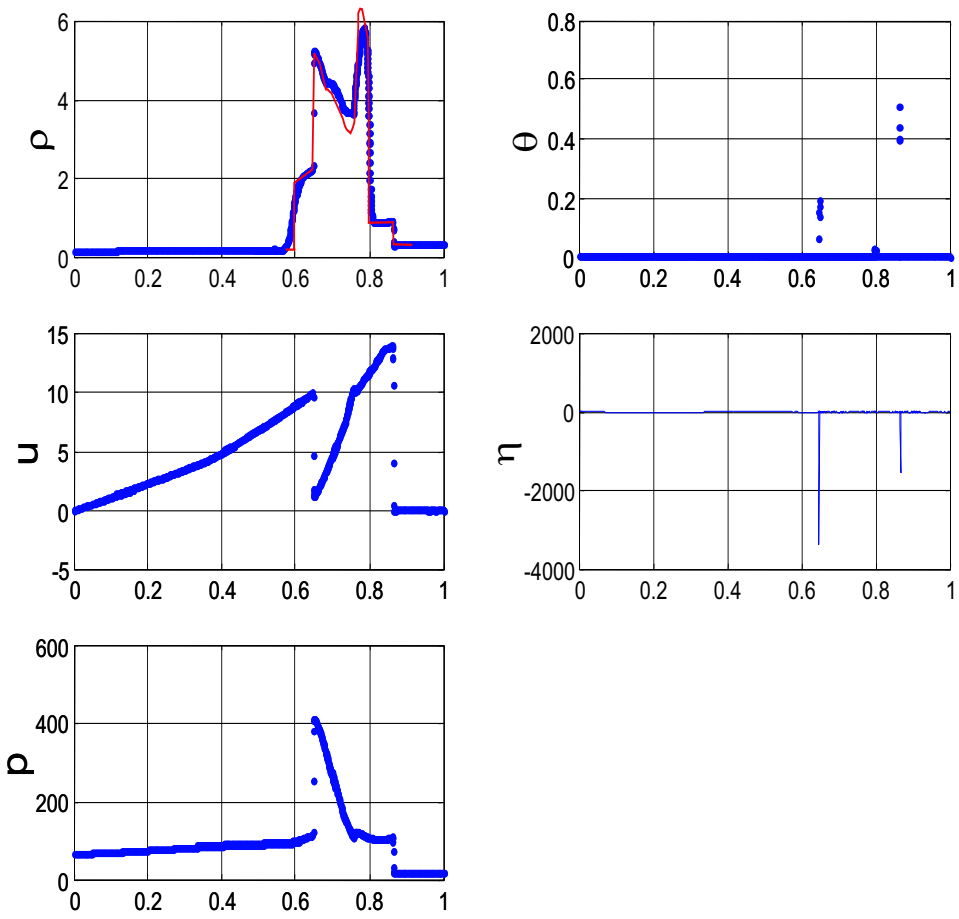

Figure 12: Woodward and Collela interacting blast waves problem

accurate results for this problem, we need to relax the constraint

$$\eta_j^{n+1} \leq 0$$

by the following one

$$\eta_j^{n+1} < \delta^n, \tag{62}$$

with δ^n equal to $3\,10^{-4}\,||\eta^n||_\infty$ for that case. By this way, we authorize the numerical method to slightly violate the principle of dissipation by convexity. At the numerical point of view, this violation generates instabilities, but spurious oscillations stay under control and do not pollute the numerical solution.
On the density profile of figure 12, we compare our numerical solution with that obtained by the PPM (piecewise parabolic) method, drawn in red solid line. Liska and Wendroff [30] have experimentally demonstrated that, among the classic methods, the PPM one gives the best results for this problem. We can see that, using (62), our numerical solution is not so far from the PPM one.

6.8 Pure water shock tube problem

This test was proposed by Cooke and Chen in [7] and Ivings, Causon and Toro in [25]. We want to illustrate that the present scheme can deal accurately with fluids like compressible water, while still providing very low effort of computation. As model of compressible water, we choose the Tait equation of state, which is often used to describe pure water for a pressure near 1 atm and a temperature near 20^o C. This equation has the form

$$p(\rho) = B\left[\left(\frac{\rho}{\rho_0}\right)^\alpha - 1\right]. \tag{63}$$

Because the pressure only depends on the density, we only consider the two equations of conservation of mass and momentum. The adiabatic exponent (see In [24]) is here given by

$$\gamma \;=\; \frac{\rho}{p}\,\frac{dp}{d\rho} \;=\; \alpha\left(1+\frac{B}{\rho}\right).$$

We suppose that B and α are constant. We take $B = 299.6$ MPa, $\rho_0 = 997.048$ kg.m^{-3} and $\alpha = 7.2$ (cf [7], [25]). The initial conditions of the Riemann problem here are

Left state	Right state
$\rho_l = 1037.8$	$\rho_r = 997.94$ $(kg.m^{-2})$,
$u_l = 0$	$u_r = 0$ $(m.s^{-1})$.

Corresponding left and right pressures are (by (63)) $p_l = 100.16$ MPa and $p_r = 1.935$ MPa. Notice that, with such initial conditions, the value of γ can reach over 1000. We present results at the final physical time $T = 2\,10^{-4}$ s, as in [7]. On figure 13, we show the numerical results using $S(U) = \frac{1}{2}||U||^2$, a 100 points uniform mesh and a CFL number equal to 0.5. The density profile we obtain is comparable to those obtained by usual schemes (Roe, HLLE,...) and relaxed versions of them (see the paper of [24] for a comparison of those results). Because the solution is only made of constant regions separated by shocks, we conclude that our scheme has the same accuracy of capture of discontinuities than other well-known schemes. The control of dissipation by the parameter θ allows us to considerably reduce the numerical dissipation of the Modified Lax-Friedrichs scheme. Again the θ parameter "switches" across the strong gradient regions to avoid oscillations. Again, we emphasize that the implementation of that method is quite easy (the complete shock tube code programmed in Matlab requires about 60 lines of code!). We do not need to find Roe matrices or analytic expressions of rarefaction or shock curves. We only need to perform flux evaluation for defining the numerical flux. The effort to adapt the source code from a polytropic gas to this pure water model is very weak.

On figure 14, we experiment the method on the same problem but we here use 400 mesh points. Our result tends to show again that the method is stable on a quite fine grid. On the other hand, the discrete shock waves are more smeared. We have compared this result with that obtained using the systematic Rusanonv scheme [40] for which the implementation is also easy (figure 15). But our hybrid scheme clearly gives better results.

6.9 Nonsmooth tabulated equation of state

To demonstrate that the method can also deal with systems with tabulated equations of state (EOS), we here consider the Euler equations with a nonsmooth EOS built as follows. Let us first denote by

$$\varphi^1(\{x_i\}_{i=1,M}, \{y_i\}_{i=1,M}; x)$$

the piecewise linear function of variable x such that $y_i = \varphi^1(.,.; x_i)$ and

$$\varphi^1_{|]x_i,x_{i+1}[} \in P^1.$$

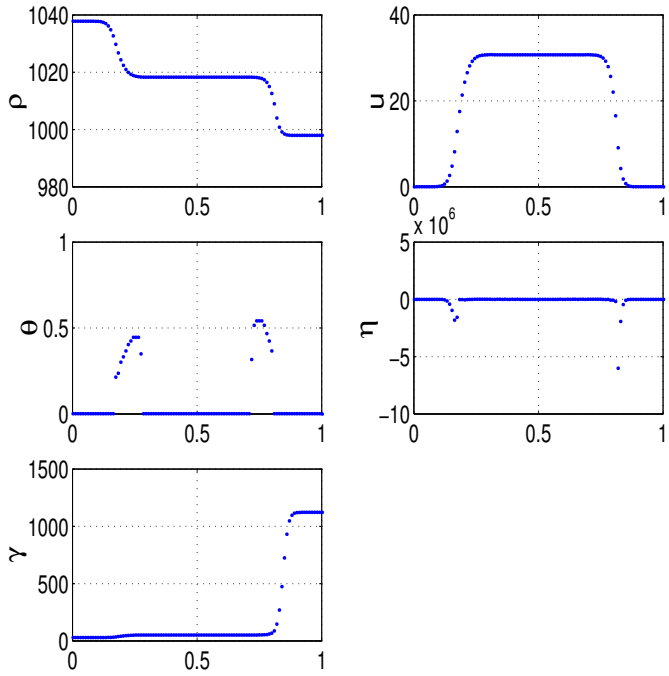

Figure 13: Two-equations pure water problem with Tait equation of state

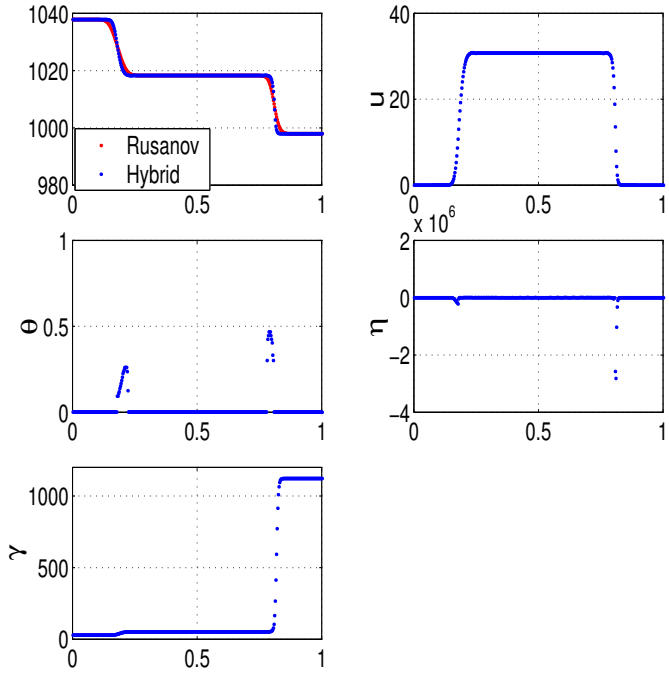

Figure 14: Same test, except 400 mesh points are used (CFL=0.5)

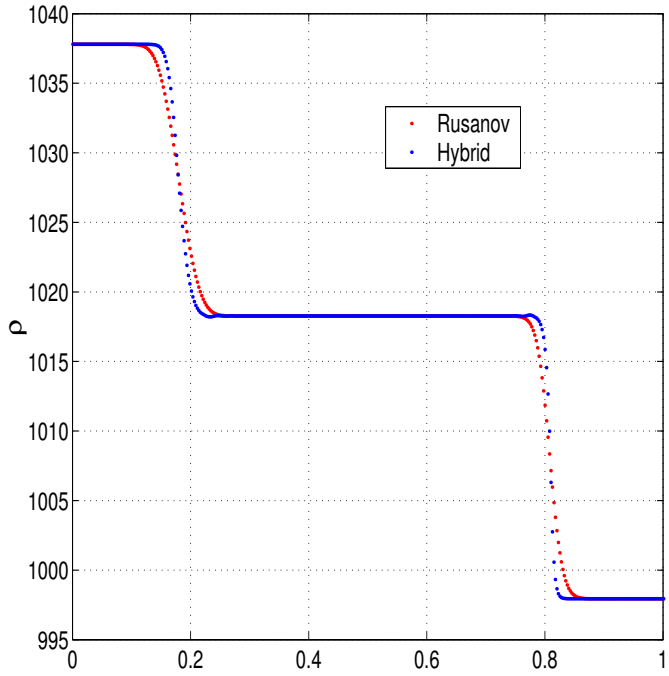

Figure 15: Comparison of the density profile between Rusanov and hybrid scheme, 400 mesh points, CFL=0.5

We consider the following EOS

$$\frac{p}{\rho} = \varphi(e), \tag{64}$$

$$\varphi(e) = \varphi^1(\{0, 2.25, 5\},\ \{0, 0.9, 6.4\}; e) \tag{65}$$

where $e = (\rho E - \frac{1}{2}\rho u^2)/\rho$ denotes the specific internal energy. This EOS has no physical meaning and is only used for the numerical interest and validation. However, some models of fluids with change of phase lead to EOS with discontinuous derivatives (transition of phase of order 0). On figure 16, we plot the graph of the function φ. In particular, the equation of state is not differentiable at point $e = 2.25$. The slopes of the function φ are constant, respectively equal to 0.4 and 2 at each side of that point. With this test case, we want to observe in particular how the method behaves in nonsmooth regions, so that we choose initial states such that the structure of the solution crosses the nondifferentiability region. We

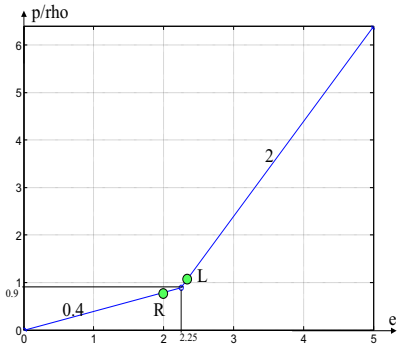

Figure 16: Tabulated equation of state for this test case

propose as initial states for the shock tube problem

Left state	Right state
$\rho_l = 1$	$\rho_r = 0.125,$
$u_l = 0$	$u_r = 0,$
$p_l = 1$ $(e = 2.3)$	$p_r = 0.1$ $(e = 2)$

(their position left (L) and right (R) is indicated on the figure 16). We perform the experiment with the following parameters: $\epsilon = -10^{-6}$, $S(U) = \frac{1}{2}||U||^2$, $CFL = 0.5$, 100 mesh points, $T = 0.2$. On figure 17, we present the numerical results. Notice that, in the case of nondifferentiable EOS, the solution is made of more than 3 waves (due to jumps on speed of sound). The numerical solution is stable and the results are reasonably accurate. The profile of function (p/ρ) at time T shows that the numerical solutions crosses the region of nondifferentiability three times.

6.10 Four equations two-phase flow Ransom faucet problem

The following test, which is due to Ransom [37] consists of a vertical water jet, contained within a cylindrical channel 12 m in length. In this section, the index g means "gas" and l means "liquid". The liquid is accelerated under the action of the gravity. At the initial state, the pipe is filled up with a uniform column of water surrounded by stagnant air, such that the gas void fraction is $\alpha_g = 0.2$ and the column has uniform water velocity of $u_l = 10$ m/s and a uniform pressure of $p = 10^5$ Pa. The boundary conditions are specified velocities of $u_l = 10$ m/s for the liquid and $u_g = 0$ m/s for the gas at the inlet,

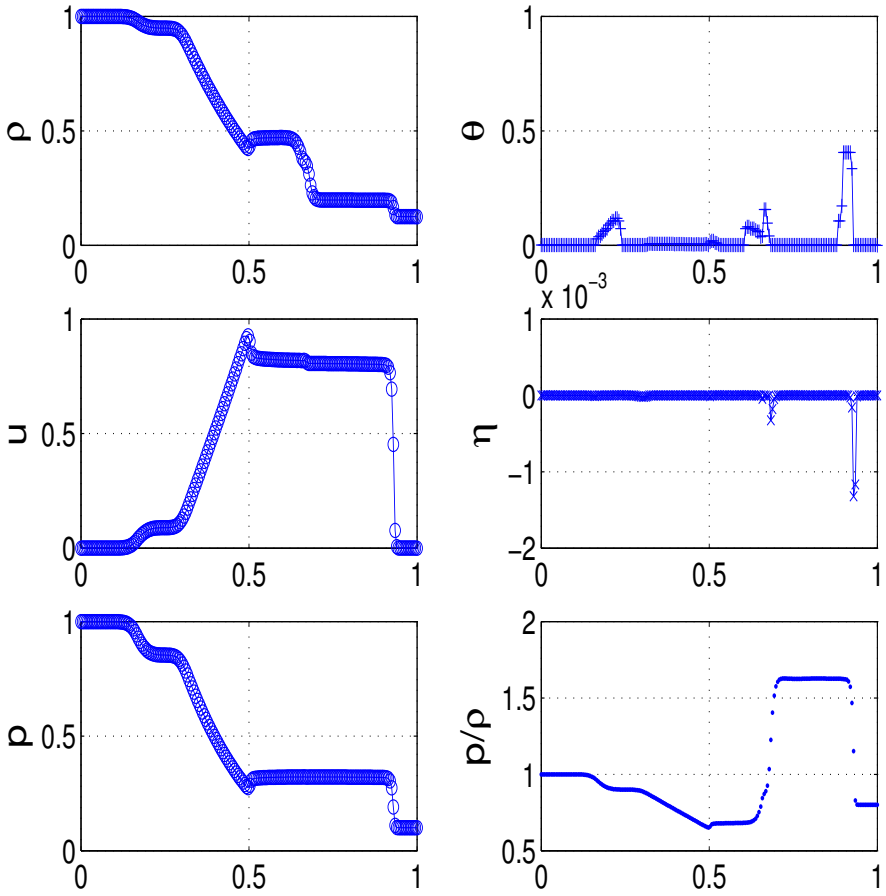

Figure 17: Shock tube problem with nonsmooth tabulated equation of state, numerical solution, $CFL = 0.5$, final time $T = 0.2$, 200 mesh points

and constant pressure $p = 10^5$ Pa at the outlet. This is a time-varying test case. At the beginning of the nonstationary phase, a void fraction waves creates and propagates downstream. Once this wave left the computational domain, we obtain a steady state. Several stages of the nonstationary process are depicted in Fig. 18.

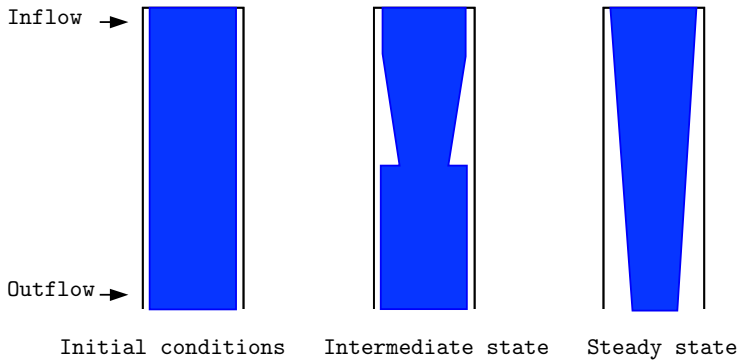

Figure 18: Water faucet problem

The analytical solution of this problem at time $T = 0.6$ can be written making some further idealisation (see [37]). More precisely, under the assumption that the liquid is incompressible and the pressure variation in gas is zero, one can get the exact solution for the evolution of the gas volume fraction

$$\alpha_g(x,t) = \begin{cases} 1 - \frac{(1-\alpha_g^0)u_l^0}{\sqrt{2gx+(u_l^0)^2}}, & x \leq u_l^0 t + \frac{gt^2}{2}, \\ 0.2, & \text{otherwise}, \end{cases}$$

where α_0^g is the initial gas volume fraction, u_l^0 the initial liquid velocity, $g = 9.81$ the gravity acceleration. We compare the gas void fraction of this exact solution to numerical results with an increasing number of mesh points: we do three numerical experiments with 80, 160 and 320 points on a uniform grid using the proposed hybrid scheme. We consider the one-dimensional four equations model two-fluid system:

$$\partial_t U + \partial_x F(U) + B(U)\partial_x U = S(U), x \in \mathbb{R},\ t > 0, \tag{66}$$

$$U(x,0) = U^0(x), \tag{67}$$

where $U = (\alpha_g\rho_g, \alpha_g\rho_g u_g, \alpha_l\rho_l, \alpha_l\rho_l u_l)$, $F(U) = (\alpha_g\rho_g u_g, \alpha_g(\rho_g u_g^2 + p), \alpha_l\rho_l u_l, \alpha_l(\rho_l u_l^2 + p))$ is the flux, $B(U)\partial_x U = (0, -p\,\partial_x(\alpha_g), 0, -p\,\partial_x(\alpha_l))$ is a nonconservative term and $S(U) = (0, \alpha_g\rho_g\, g, 0, \alpha_l\rho_l\, g)$ is the source term of force due to gravity. The conservation of the mass of the global mixture imposes

$\alpha_g + \alpha_l = 1$. Finally, we choose an isentropic model for both gas and liquid phases. For this four equation single pressure model, we choose for each phase a stiffened gas equation of state (see [2] for example):

$$p_k = (\gamma_k - 1)\rho_k e_k - \gamma_k \pi_k, \ k = g, \, l, \tag{68}$$

where p_k and e_k respectively denote the pressure and the internal energy of each phase, γ_k is a dimensionless constant and π_k is a constant "shift" pressure. We more suppose that each phase has an isentropic evolution, that means that

$$T_k d\, s_k \ = \ 0 \ = \ de_k - \frac{p_k}{\rho_k^2}\, d\rho_k, \ k = g, \, l, \tag{69}$$

where T_k and s_k respectively denote the temperature and the specific entropy of each phase k. Combining equations (68) and (69) gives the law

$$p_k \ = \ A_k \rho_k^{\gamma_k} - \pi_k. \tag{70}$$

For the numerical solution of the problem, the parameters of the stiffened gas equation of state were taken as follows,

$$\begin{array}{cc} \text{Liquid} & \text{Gas} \\ \gamma_l = 4.4 & \gamma_g = 1.4, \\ \pi_l = 6 \cdot 10^6 & \pi_g = 0. \end{array} \tag{71}$$

In addition, constants A_k were designed in such a way that, for $p = 10^5$ Pa, we have $\rho_l = 1000 \ kg\, m^{-3}$ and $\rho_g = 1.286 \ kg\, m^{-3}$. That leads to the following constant values:

$$\begin{array}{cc} \text{Liquid} & \text{Gas} \\ A_l = 3.84883980133 \cdot 10^{-7} & A_g = 7.0317374052 \cdot 10^4. \end{array} \tag{72}$$

In the numerical experiment, we use $S(U) = \frac{1}{2}||U||^2$, what can appear far from being a good choice because the components of S have not the same dimension. Contrary to the compressible Euler equations for a perfect gas, the system of equations (66) cannot be rewritten into a dimensionless system. Moreover, the system is very stiff regarding the coefficients (71) and (72) of the equations of state. For that reason, one could ask if it is really reasonable to use the convex function $\frac{1}{2}||U||^2$ because of the heterogeneous dimensions and scales of the components of U. Remark however that the expression of η_j^{n+1} which is the real quantity of interest only involves differences of the form ΔS and $\lambda \nabla_U S \cdot \Delta F$, but (symbolically)

$$\Delta S \ = \ \sum_k \Delta \left((U_k)^2 \right) \ = \ \sum_k \bar{U}_k \ \Delta U_k$$

and

$$\lambda \nabla_U S \cdot \Delta F \;=\; \lambda U \cdot \Delta F \;=\; \lambda \sum_k U_k \, \Delta F_k,$$

where k denotes all the components of vector U. Thus, the component decomposition of the term η_j^{n+1} shows that each component compares terms of the same dimension and order.

For the numerical discretization of both nonconservative and source terms, we use the approach exposed in sections 5.2 and 5.1. On the respective figures 19, 20 and 21, we present the numerical solutions at the fixed time $T = 0.6s$ using respectively 80, 160 and 320 discretization points. On each figure are plotted the profiles of gas void fraction α_g, pressure p, gas velocity u_g, liquid velocity u_l, coefficient θ and local dissipation η. On the gas fraction, we also draw the exact solution with green solid line.

We emphasize that we do not use hyperbolicity correction terms like those proposed by Bestion [5] for our computations.

The numerical results are quite satisfactory, but difficulties still persist. On figure 19, a uniform grid on 80 points is used. The Courant number is kept constant, equal to 0.3. We observe that the numerical solution do not produce oscillations. The void fraction wave is spread out on lot of points, but the accuracy we obtain is far better than the one obtained by classical upwind schemes (see [10], [11] or [16] for example) at equivalent mesh. This only requires a few minutes of computational time on a CPU 600 Mhz personal computer. Remark that the maximum value of θ within the computational domain is of the order of 0.02, which explain the great accuracy and the quasi second order accuracy.

What is still not satisfactory in this computation is the oscillatory behaviour of the θ field, even if we use very small increments $\Delta\theta_j^{n,k}$ (see the comments in the nozzle flow section). Although the profile of θ smoothly grows up between times 0s and $0.2s$, it begins to oscillate after time $t = 0.2s$ and oscillations also evolve during time.

This behaviour is more strongly observed using 160 mesh points. The noisy behaviour of θ tends to create oscillations on the pressure and on the gas velocity profiles. Surprisingly, the profiles of gas void fractions and liquid velocity profiles are not sensible to the noisy behaviour of θ. Here, a CFL number of value 0.4 is used and seems to be the limit of stability.

When using 320 mesh points and a CFL number of 0.3 (see figure 21), we observe a small oscillation on

α_g around $x = 2.3$ that we cannot interpret. One can see an undershoot at the foot of the void fraction wave wich is due to a loss of hyperbolicity in this region. Nevertheless, the undershoot remains small. What is remarkable in this computation is the accurate capture of the void fraction wave. The profile of θ_j^n is still so noisy. A consequence is that our numerical flux suffers from a lack of regularity and does not respect the assumptions of regularity of conventional theorems of convergence.

Seeing these results, we still do not know if our method really converges. What we say is that the method is performing when coarse grids are used. Practically, only coarse grids are utilized for two-phase flows because of the heavy computational costs they involve. When the mesh size h tends to zero, perhaps we are confronted to a problem of stability analogous to the Gibbs phenomenon in polynomial interpolation : the method stay accurate but the amplification coefficient depends on h and diverges when h tends to zero. At the present time, we do not have the answer. This is at the aim of future theoretical works.

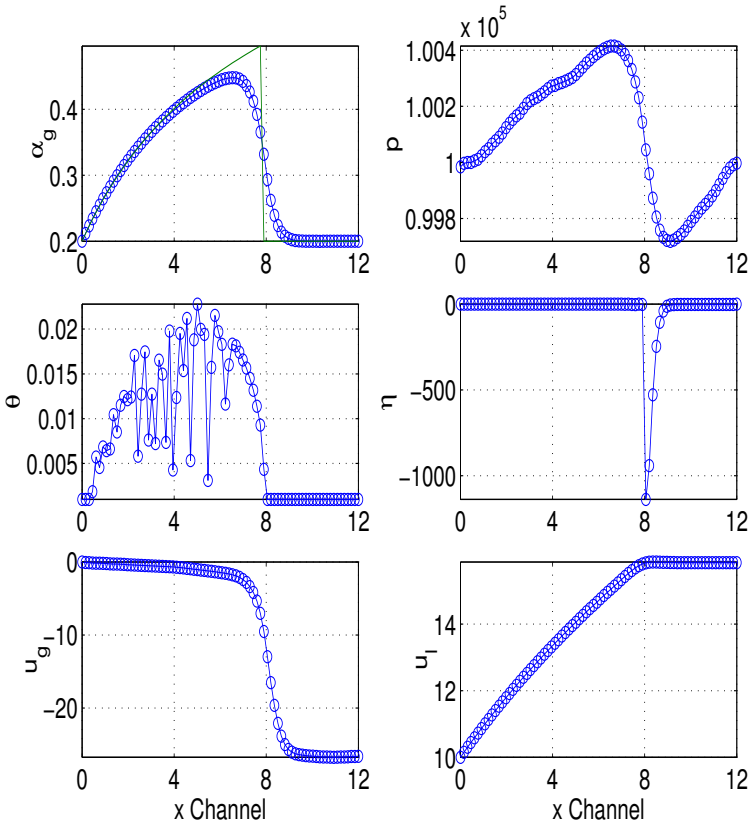

Figure 19: Numerical results. Numerical solution computed on a 80 points uniform grid, CFL=0.3 at time T=0.6. The exact solution for α_g is also plotted in green solid line.

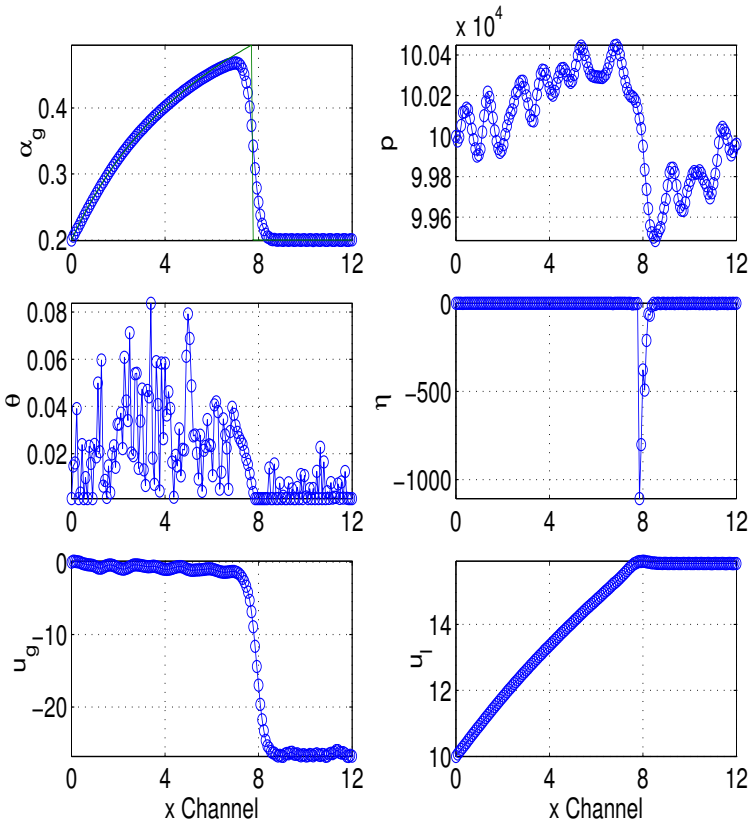

Figure 20: Numerical results. Numerical solution computed on a 160 points uniform grid, CFL=0.4 at time T=0.6.

6.11 Two-dimensional shock reflection problem

We study the reflection of an oblique shock on the lower side of a rectangular domain defined by $0 \leq x \leq 4.12829$, $0 \leq y \leq 1$. We consider the two-dimensional compressible Euler equations:

$$\partial_t U + \partial_x F(U) + \partial_y G(U) = 0, \tag{73}$$

$$U(x, y, 0) = U^0(x, y), \tag{74}$$

with $U = (\rho, \rho u, \rho v, \rho E)$. The fluxes $F(U)$ and $G(U)$ are defined by

$$F(U) = (\rho u, \rho u^2 + p, \rho uv, (\rho E + p)u), \quad G(U) = (\rho v, \rho uv, \rho v^2 + p, (\rho E + p)v).$$

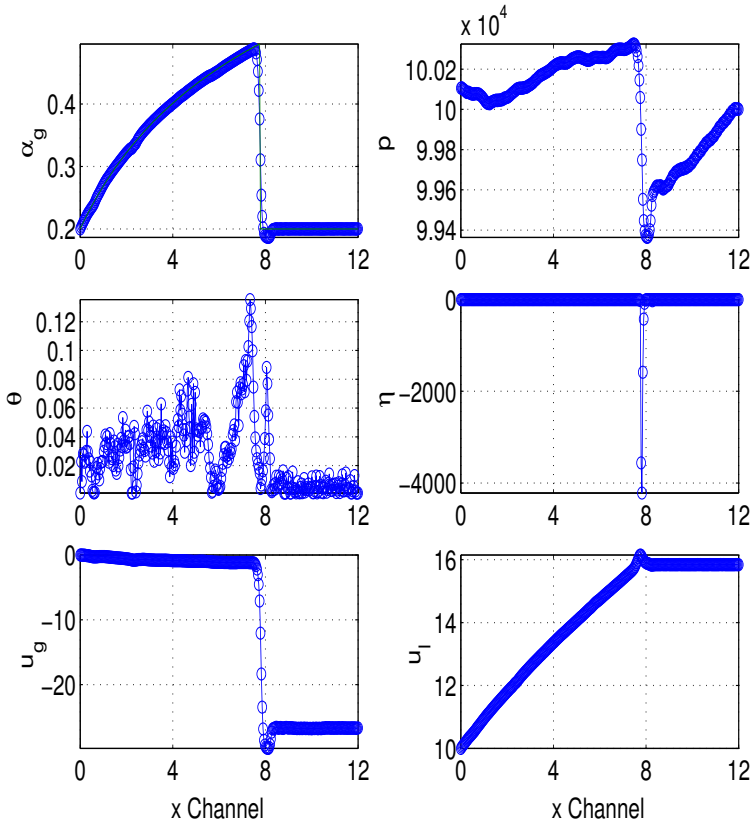

Figure 21: Numerical results. Numerical solution computed on a 320 points uniform grid, CFL=0.3 at time T=0.6. Some undershoot at the foot of the void fraction wave appears because of the loss of hyperbolicity.

The variables u and v are components of the velocity field $\vec{u}$. The gas is assumed to be perfect and polytropic with pressure $p = (\gamma - 1)(\rho E - \frac{1}{2}\rho(u^2 + v^2))$, $\gamma = 1.4$. The initial flow is given

$$\rho = 1,\ u = 2.9,\ v = 0 \text{ and } p = \frac{1}{1.4}.$$

The boundary conditions are the following:

- inflow boundary conditions on $x = 0$, all the variables are fixed taking the same values as at initial time (supersonic inflow);
- outflow boundary conditions on the side $x = 4.12829$, no variable is imposed (supersonic outflow);
- fixed values on the upper side $y = 1$ (those of the exact stationary solution):

  $$\rho = 2.68732,\ u = 2.40148,\ v = 0 \text{ and } p = 2.93413;$$

  wall reflection conditions on the lower side $y = 0$;
- the numerical treatment of the wall boundary condition is performed by adding an horizontal line of "ghost mirror cells" with opposite v-velocity components. Then the numerical flux is used through wall edges.

Finally, a uniform cartesian mesh is used with respective component mesh space steps $h_x = 4.12829/80$ and $h_y = 1/25$ ($80 \times 25 = 2000$ cells). Again in this numerical experiment, we use the simple convex

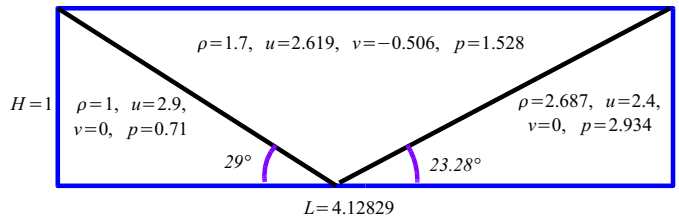

Figure 22: Description and solution of the stationary shock reflection problem

function $\tilde{S}(U) = \frac{1}{2}\,||U||_2{}^2$. The numerical "steady state" is presented below. What we can see is that the numerical method captures the solution with a good accuracy. In fact, at "convergence", the maximum value of θ within the computational domain is 0.3 which explains the weak amount of numerical dissipation.

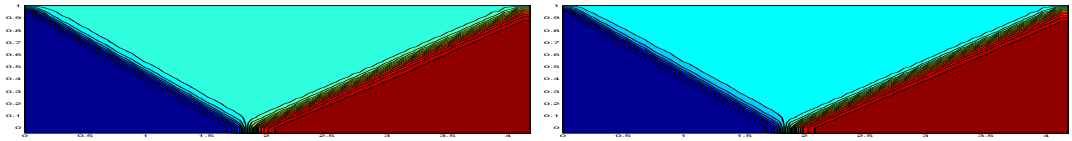

Figure 23: Steady state numerical solution. Iso-contours of density ρ and pressure p.

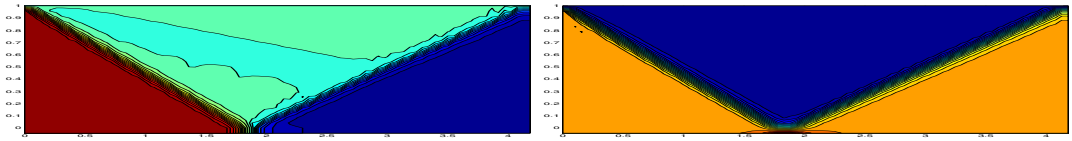

Figure 24: Steady state numerical solution. Iso-contours of the two components of the velocity u and v.

6.12 Downloading source codes

Source codes of the previous numerical experiments written in Matlab can be downloaded and freely used at the following URL : *http://www.mas.ecp.fr/labo/equipe/devuyst/hybrid/*.

7 Conclusion and future works

In this exploratory work, we have analyzed an hybrid "central scheme-like" scheme with an original approach for computing the hybridization coefficients θ. This is based on computing the smallest value $\theta \in [0, 1]$ that respects the local numerical dissipation inequality

$$\eta_j^{n+1}(\theta_j^n) \ \leq \ 0$$

which depends on the choice of a certain convex function $S(U)$. This convex function is not necessary a mathematical entropy in the sense of Lax. This is an interesting feature especially for "complex" systems where it is difficult (see impossible) to find an (entropy-entropy flux) pair. Of course, we think

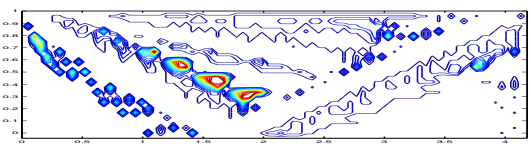

Figure 25: Steady state numerical solution. Iso-contours of coefficients θ.

of applications of two-phase flow where averaged models do not always admit entropy pairs.

More, we remark that we can approximate as close as we want the Lax-Wendroff flux without computing the Jacobian matrix of the flux. Consequently, the hybrid flux, which is a combination of the modified Lax-Friedrichs flux and the approximate Lax-Wendroff flux does not need to compute any derivative or Jacobian matrix. This is an interesting feature for fast implementation and rapid prototypying purposes. This can also be interesting when one deals with physical fluxes that are not continuously differentiable (only locally Lipschitz continuous). This lack of of regularity can occur again in the framework of two-phase flows (see for example [13] about this question for Homogeneous Equilibrium HEM Models).

The numerical results presented in the paper are not superior to many existing state-of-the-art numerical methods for conservation laws such as ENO, MUSCL or central scheme of Tadmor and coworkers. The interest is rather the systematic feature of the method and its very fast implementation for prototypying and fluid model validation. In this context, the Rusanov scheme is today often used; the present approach seems to give better results. We believe that this kind of schemes can be an alternative of the family of upwind schemes in the multiphase flow framework. We have numerically shown that the method can solve nonstationary as well as stationary problems in one or two space variables. For stationary problems, we still have difficulties of convergence to the steady state, due to the iterative process of the computation of θ. Let us mention that we could had used Newton's fixed point method for computing θ, but this has not been implemented in this exploratory work.

We have performed a first extension of the method to the case of nonhomogeneous equations or in the presence of nonconservative products. The method gives very accurate results on the Ransom faucet problem, especially for the capture of the void fraction wave. But the field of the combination coefficients θ is quite noisy and leads to nonsmooth numerical flux. Seeing these results, we still do not know if our method really converges. What we say is that the method is performing when coarse grids are used. Practically, only coarse grids are utilized for two-phase flows because of the heavy computational costs they involve. When the mesh size h tends to zero, perhaps are we confronted to a problem of stability : the method is consistent but due to a possible loss of weak stability in a weak space (BV for example), it diverges when h tends to zero. At the present time, we do not have the answer.

In future works, we will deal to the extension of such a method to multidimensional problem using (if it

is possible) unstructured Finite Volumes. The theoretical question of the convergence in our case has to be understood.

References

[1] F. Benkhaldoun, *Analysis and validation of a new finite volume scheme for nonhomogeneous systems*, Proceedings of the Third int. Symp. on Finite Volumes for Complex Applications FVCA 3, R. Herbin, D. Kröner Eds., HPS, 2002, pp. 269-276.

[2] N. Andrianov, R. Saurel and G. Warnecke, *A simple method for compressible multiphase mixtures and interfaces*, INRIA Technical Report RR-4247 (2001), *ftp://ftp.inria.fr/INRIA/publication/publi-pdf/RR/RR-4247.pdf*.

[3] M. Baudin, C. Berthon, F. Coquel, Ph. Hoche, R. Masson, Q.H. Tran, *A relaxation method for two-phase flow models with hydrodynamic closure law* (2002), to appear.

[4] J.P. Boris and D.L. Book, *Flux corrected transport I*, SHASTA, a fluid transport algorithm that works, J. Comp. Phys., 11 (1973), pp. 38-89.

[5] D. Bestion, *The physical closure laws in the CATHARE Code*, Nucl. Eng. Design, 124 (1990), pp. 229-245.

[6] F. Bouchut, *An antidiffusive entropy scheme for monotone scalar conservation laws* (2002), preprint, *http://www.math.ntnu.no/conservation/2002/051.html*

[7] C.H. Cooke and T.J. Chen, *On shock capturing for pure water with general equation of state*, Comm. Appl. Numer. Methods, 8 (19920, pp. 219-233.

[8] P. Collela, *A direct Eulerian MUSCL scheme for gas dynamics*, SIAM J. Sci. Stat. Comput., 6 (1985), pp. 104-117.

[9] F. Coquel, M.S. Liou, *Hybrid upwind splitting (HUS) by a field-by-field decomposition*, NASA TM-106843, Icomp-95-2 (1995).

[10] J. Cortes, *On the construction of upwind schemes for nonequilibrium transient two-phase flows*, Computers & Fluids (2002), pp. 159-182.

[11] P.H. Cournede, B. Desjardins, A. Llor, *A TVD Lagrange plus remap scheme for the simulation of two-fluid flows*, Proceedings of the Third int. Symp. on Finite Volumes for Complex Applications FVCA 3, R. Herbin, D. Kröner Eds., HPS, 2002, pp. 495-502.

[12] F. Coquel, B. Perthame, *Relaxation of energy and approximate riemann solvers for general pressure laws in Fluid Dynamics*, SIAM J. Numer. Anal. 35(6) (1998), pp 2223-2249.

[13] F. De Vuyst, J.M. Ghidaglia, G. Le Coq, *On the numerical simulation of multiphase water flows with changes of phase and strong gradients using the Homogeneous Equilibrium Model*, submitted to Int. J. Mult. Flows, (2002), *http://www.math.ntnu.no/conservation/2002/057.html*

[14] S.K. Godunov, *A difference scheme for numerical computation of discontinuous solutions of equation of fluid dynamics*, Mat. Sbornik, 47(89) (1959), pp. 271-306.

[15] E. Godlewski, P.A. Raviart, *Hyperbolic systems of conservation laws*, Mathématiques et Applications, Ellipses (1991), ISSN 1154-483 X.

[16] K. Halaoua, *Quelques solveurs pour les opérateurs de convection et leurs applications la mcanique des fludies diphasiques*, PhD Thesis and *publication du CMLA*, ENS de Cachan, France (1998)

[17] A. Harten and P.D. Lax, *A random choice finite difference scheme for hyperbolic conservation laws*, SIAM Jour. Numer. Anal., 18 (1981), pp. 289-315.

[18] A. Harten, P.D. Lax and B. van Leer, *On upstream differencing and Godunov-type schemes for hyperbolic conservation laws*, SIAM Review, 25 (1983), pp. 35-61.

[19] T. Hou and Ph. Le Floch, *Why nonconservative scheme do not converge to weak solutions*, Math. Comp., 62(206), (1994), pp. 497-530.

[20] A. Harten and G. Zwas, *Seft-adjusting hybrid schemes for shock computation*, J. Comp. Phys., 9 (1972), pp 568.

[21] T. Gallouët, J.M. Hérard, N. Seguin, *Some recent Finite Volume Schemes to compute Euler equations using real gas EOS*, Internat. J. Numer. Methods Fluids, Vol. 39-12 (2002), pp. 1073-1138.

[22] J.M. Ghidaglia, A. Kumbaro, G. Le Coq, *On the numerical solution of two fluid models via a cell centered Finite Volume method*, Eur. Jour. Mech. B/Fluids, vol. 20(6) (2001) pp. 841-867.

[23] E. Godlewski and P.A. Raviart, *Numerical approximation of hyperbolic systems of conservation laws*, Appl. Math. Sci. 118, Springer (1996)

[24] A. In, *Numerical evaluation of an energy relaxation method for inviscid real fluids*, Siam J. Sci. Comput., vol. 21 (1), PP. 340-365 (1999).

[25] M.J. Ivings, D.M. Causon and E.F. Toro, *Riemann solvers for compressible water*, Proc. ECCOMAS 1996, John Wiley, New York, 1996.

[26] S. Jin, Z. Xin, *The relaxation scheme for systems of conservation laws in arbitrary space dimension*, Comm. Pure Appl. Math., 45 (1995), pp 235-276.

[27] A. Kurganov and E. Tadmor, *New high resolution central schemes for nonlinear conservation laws and convection-diffusion equations*, J. Comp. Phys., 160 (2000), pp. 241-282.

[28] P.D. Lax , *Shock waves and entropy*, in *Contributions to nonlinear functional analysis*, E.A. Zarantonello (Ed.), Academic Press, NY (1971), pp. 603-634.

[29] P.D. Lax and B. Wendroff, *Systems of conservation laws*, Comm. Pure Appl. Math., 13 (1960), pp. 217-237.

[30] R. Liska and B. Wendroff, *Comparison of several difference schemes on 1D and 2D test problems for the Euler equations*, submitted to SISC SIAM J. Sci. Comput. (2003).

[31] R. Liska and B. Wendroff, *Composite schemes for conservation laws*, SIAM J. Numer. Anal., 35(6), pp. 2250-2271 (1998).

[32] R. W. MacCormack, *The effect of viscosity in hypervelocity impact cratering*, AIAA Paper 69-354, 1969.

[33] A. Majda, S. Osher, *A systematic approach for correcting nonlinear instabilities*, Numer. Math., 30 (1978), pp. 429-452.

[34] H. Nessyahu and E. Tadmor, *Non-oscillatory central differencing for hyperbolic conservation laws*, JCP, vol. 87, pp. 408-463 (1990).

[35] S.J. Osher, *Riemann solvers, the entropy condition, and difference approximations*, SIAM J. Numer. Anal., 21, pp. 217-235 (1984).

[36] S.J. Osher, *Convergence of generalized MUSCL schemes*, SIAM J. Numer. Anal., 22 (5), pp. 947-961 (1985).

[37] V.H. Ransom, *Numerical tenchmark tests*, in G.F. Hewitt, J.M. Delhaye and N. Zuber, Eds, *Multiphase Science and Technology*, 3, Hemisphere Publishing Corporation (1987).

[38] R.D. Richtmyer and K. W. Morton, *Difference methods for initial-value problems*, Wiley-Interscience, 1967.

[39] P.L. Roe, *Approximate Riemann solvers, parameter vectors and difference schemes*, J. Comp. Phys. 43 (1981), pp. 357-372.

[40] V.V. Rusanov, *Calculation of interaction of non-steady shock waves with obstacles*, J. Comp. Math. Phys. USSR, vol. 1 (1961), pp. 267-279.

[41] M. Schonbeck, *Second-order conservative schemes and the entropy condition*, Math. Comp., 44 (1985), PP. 31-38.

[42] G. Sod, *A survey of several finite difference methods for systems of nonlinear hyperbolic conservation laws*, J. Comput. Phys., 27 (1978), pp. 1-31.

[43] P. Woodward and P. Colella. *The numerical simulation of two-dimensional fluid flow with strong shocks*, J. Comp. Phys., 54, pp. 115-173, (1984).

[44] S.T. Zalesak, *Fully multidimensional flux corrected transport algorithms for fluids*, J. Comp. Phys., 31 (1979), pp. 335-362.